

The Empirical Low Energy Ion Flux Model for the Terrestrial Magnetosphere

William C. Blackwell*

Jacobs Engineering, Marshall Space Flight Center Group, Huntsville, AL 35812 USA

Joseph I. Minow†

NASA Marshall Space Flight Center, Huntsville, AL 35812 USA

Anne M. Diekmann‡

Jacobs Engineering, Marshall Space Flight Center Group, Huntsville, AL 35812 USA

The Living With a Star Ion Flux Model (IFM) is a radiation environment risk mitigation tool that provides magnetospheric ion flux values for varying geomagnetic disturbance levels in the geospace environment. IFM incorporates flux observations from the Polar and Geotail spacecraft in a single statistical flux model. IFM is an engineering environment model which predicts the proton flux not only in the magnetosphere, but also in the solar wind and magnetosheath phenomenological regions. This paper describes the ion flux databases that allows for IFM output to be correlated with the geomagnetic activity level, as represented by the Kp index.

I. Introduction

Even outside of the radiation belts, spacecraft can be exposed to a significant proton flux environment. The source of the proton flux can be from the solar wind, magnetosheath, or magnetosphere regions of geospace. Episodic injections of plasma from the magnetotail during substorms and major magnetic storms can increase proton flux in the energy band of concern by orders of magnitude in the outer magnetosphere. Although at flux levels that are typically lower than seen in the magnetosphere, protons are also found outside of the magnetosphere in the dusk and dayside magnetosheath, or even upstream of the bow shock, since “leakage” across the magnetopause is one of the loss mechanisms for magnetospheric plasma. Energetic solar protons are another source of potentially damaging particles. Solar event protons are a concern not only while a spacecraft is in the solar wind, but they also pose a risk while the spacecraft is in the magnetosheath or in the outer magnetosphere. Energetic solar protons easily traverse the bow shock and magnetosheath with little variation in flux and can even penetrate the lower magnetic field regions of the outer magnetosphere.

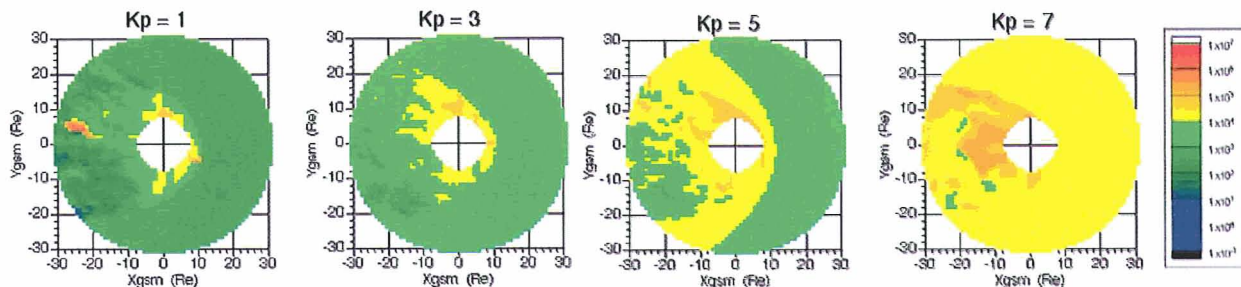


Figure 1. Sample CRM output. Kp dependent proton flux (in units of #/cm²-s-sr-MeV) given by the model for protons between 100 keV and 200 keV (adapted from Blackwell et al., 2003).

* Engineering Specialist, Jacobs Engineering, MSFC Group, MSFC/EV13, Huntsville, AL

† AST, Flight Vehicle Space Environments, Spacecraft and Vehicle Systems Department, NASA/MSFC/EV13, Huntsville, AL, Senior Member

‡ Analyst, Jacobs Engineering, MSFC Group, MSFC/EV13, Huntsville, AL

IFM addresses the need for a low energy flux model of the Earth’s magnetosphere that can be used in spacecraft design and mission analysis. This is an empirical engineering ion flux model applicable over a range of geocentric radial distances of approximately 2 Earth radii (Re) to the magnetopause within a maximum distance of 30 Re in the direction of the magnetotail. The model provides differential energy flux over a range from 58.1 keV to 1560.8 keV in 8 logarithmic energy steps. A key feature of the model is ion flux values traceable to satellite observations of the ion environment. Data is binned in spatial volume elements and sorted to yield Kp dependent flux estimates that are reported for percentile values (e.g., 50 %, 95 %) in the region.

IFM is an alternative to standard environment models such as AP-8 which are not applicable for radial distances that include the outer magnetosphere where there are strong azimuthal asymmetries in charged particle flux. In addition, the modeling approach used in creating IFM includes not only the magnetosphere, but also the magnetosheath and near-Earth solar wind particle flux in the database, since these environments are available in the datasets used to derive the model. Thus, IFM provides an integrated charged particle environment definition model useful for a variety of applications including spacecraft design analysis, near real time environment modeling, and dynamic flux estimates for use in on-orbit operations support within 30 Re of the Earth.

II. Technical Approach and Methodology

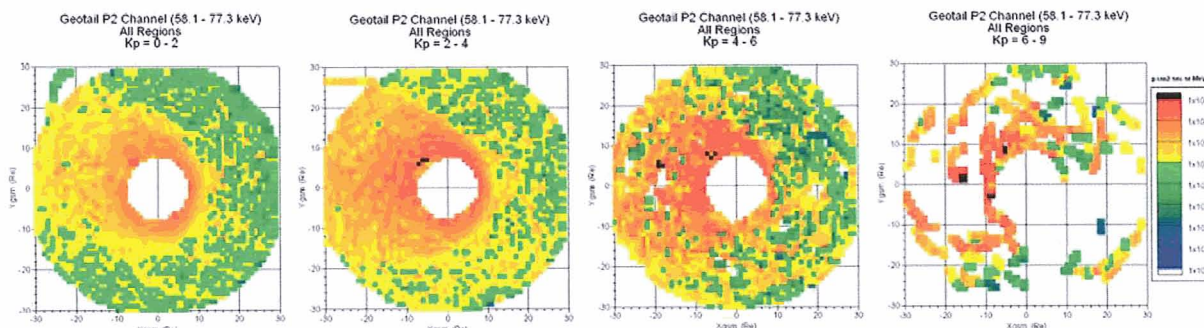


Figure 2. Low energy (58.1 – 77.3 keV) proton flux as a function of the Kp magnetic activity index.

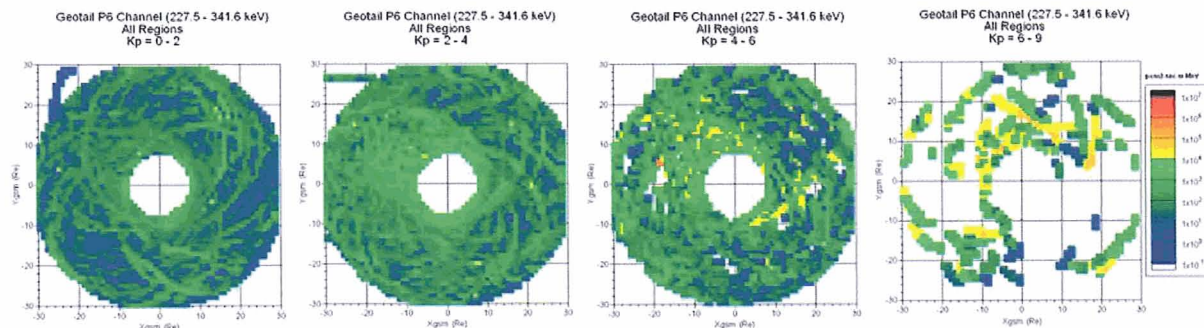


Figure 3. Medium energy (227.5 – 341.6 keV) proton flux as a function of the Kp magnetic activity index.

The development of IFM has heavily leveraged experience gained in creating the ion flux model for the Chandra X-ray observatory. The Chandra Radiation Model (CRM) was developed in response to the need for a tool to predict the 100-200 keV proton flux along its orbit [Blackwell et al., 2000, 2003]. NASA standard trapped proton AP-8 [Sawyer and Vette, 1976] and electron AE-8 [Teague and Vette, 1974; Vette, 1991] models are used by the Chandra program to determine the mean locations of the very energetic radiation belts but are not adequate to address the issue of low energy protons in the outer radiation belts. CRM is the first engineering-level ion environment model for the outer magnetosphere. CRM is designed for use both as a scheduling tool for planning science observations for periods up to three weeks and for a real-time environment model for estimating low energy proton environments. Proton flux values as a function of Kp geomagnetic activity index from the CRM Version 2 are shown in Fig. 1. IFM is an empirical ion flux model of the magnetosphere using satellite observations of ion flux. Input to the model is location in space, date and time of year, and appropriate

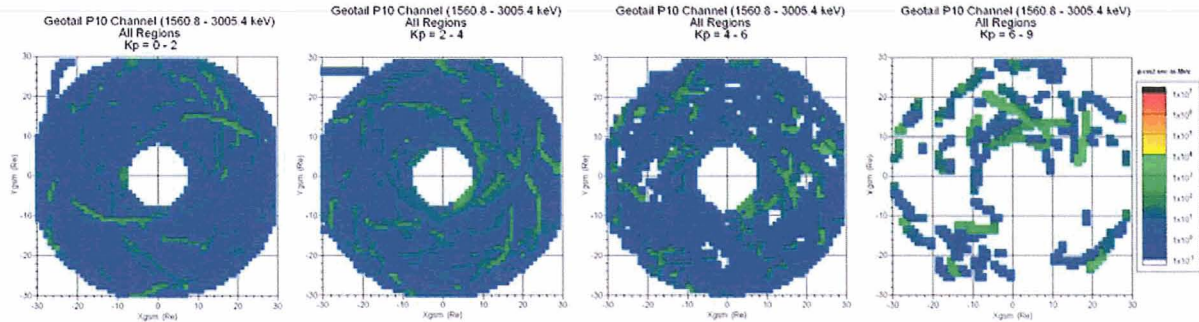


Figure 4. High Energy (1560.8 – 3005.4 keV) proton flux as a function of the Kp magnetic activity index.

interplanetary environment conditions (e.g., interplanetary magnetic field, solar wind density and velocity) and geomagnetic indices (e.g., Dst, Kp). The software returns values of the ion flux for user selected percentile levels (e.g., the maximum flux value that would be predicted to occur 50% or 95% of the time).

IFM incorporates code from two separate space environment models to calculate magnetopause and bow shock boundary locations. The magnetopause model is taken from the Tsyganenko geomagnetic field model [Tsyganenko, 1995]. The bow shock model used is one adapted from a model by Bennett et. al. [Bennett, 1997]. The original version of CRMFLX provided ion flux values as a function of Kp but was limited both in its range of spatial application ($-8 \text{ Re} < Z_{\text{GSM}} < +15 \text{ Re}$) and particle energy (100 keV to 200 keV protons) to meet specific requirements of the Chandra Program.

2.1 Model Implementation

Ion flux environments in the outer magnetosphere are complex and variable. Traditional techniques used to create trapped particle models (e.g., simple B-L flux mapping) are not applicable in magnetospheric regions where the geomagnetic field is highly perturbed and is significantly different than the dipole configuration. CRMFLX consists of a combination of analytical and database driven models, driven by proxy parameters of geomagnetic activity levels, Kp and Dst, that provide for correlation of magnetospheric particle flux with geomagnetic disturbances.

Table 1. Geotail EPIC/ICS Energy Bands

Channel Name	Species	Energy Band (keV/e)	Sector (deg)	Time Res. ^a (sec)	Time Res. Database ^b (sec)
P2	p+	58.1 - 77.3	22.5	6	288
P3	p+	77.3 - 107.4	22.5	48	288
P4	p+	107.4 - 154.3	22.5	48	288
P5	p+	154.3 - 227.5	22.5	48	288
P4	p+	107.4 - 154.3	22.5	48	288
P5	p+	154.3 - 227.5	22.5	48	288
P6	p+	227.5 - 341.6	22.5	48	288
P7	p+	341.6 - 522.5	22.5	48	288
P8	p+	522.5 - 813.5	22.5	48	288
P9	p+	813.5 - 1560.8	22.5	96	288
P10	p+	560.8 - 3005.4	22.5	96	288

^aTime resolution of original data.

^bTime resolution of spin averaged data obtained from Principle Investigator.

Figures 2-4 shows that there is good correlation between Kp and the ion flux in the outer magnetosphere. Unfortunately, the spatial regions that are sampled by spacecraft is very sparse during periods when the magnetic activity level is high (with correspondingly high ion flux). It is not possible then to have a model based strictly upon spacecraft measurement of the ion flux levels, while still having good coverage of all spatial regions of interest. Instead, the approach is a combination of database and analytical techniques that fill in the spatial gaps while at the same time maintaining a direct link to the satellite measurements.

Ion flux measurements from the Geotail and Polar spacecraft were used to create the IFM database. Geotail is in a highly elliptical orbit that lies in the equatorial plane with a perigee of 8 Earth radii (Re) and apogee of 30 Re. This orbit makes Geotail particularly useful in creating an ion flux model for the outer magnetosphere, since it can directly sample the high flux plasma sheet region. While the equatorial orbit does allow for mapping along magnetic field lines to populate a larger region of the magnetosphere than what is directly measured, the Geotail data cannot provide information to populate the higher magnetic latitudes. Fortunately, the other principal data

Table 2. CEPPAD/IPS Energy Bands

Energy Channel	Species	Energy Threshold Set 1		Energy Threshold Set 2	
		Min (keV)	Mid (keV)	Min (keV)	Mid (keV)
0	H ⁺	16.8	18.9	13.9	15.6
1	H ⁺	21.2	24.4	17.5	19.9
2	H ⁺	27.9	32.4	22.6	26.2
3	H ⁺	37.5	43.1	30.3	35.4
4	H ⁺	49.6	57.2	41.4	48.1
5	H ⁺	65.9	76.0	55.9	55.2
6	H ⁺	87.7	102.0	75.9	88.4
7	H ⁺	118.0	138.0	103.0	121.0
8	H ⁺	161.0	188.0	142.0	168.0
9	H ⁺	221.0	259.0	198.0	234.0
10	H ⁺	303.0	355.0	277.0	327.0
11	H ⁺	417.0	489.0	387.0	459.0
12	H ⁺	574.0	674.0	543.0	643.0
13	H ⁺	791.0	929.0	762.0	903.0
14	H ⁺	1091.0	1281.0	1071.0	1269.0
15	H ⁺	1505.0	2000.0	1505.0	2000.0

source for the ion flux model, the Polar spacecraft, does provide information that allows for calculations of ion flux at high magnetic latitudes in the outer magnetosphere. The Polar spacecraft is in a polar orbit (2 Re x 9 Re) which crosses all magnetic latitudes. While the Polar spacecraft's orbit does not directly sample the outer magnetosphere (> 9 Re), its data can be mapped along magnetic field lines to more completely fill the magnetosphere.

Ion flux measurements used in creating the IFM database are from the Energetic Particles and Ion Composition (EPIC) Ion Composition Subsystem (ICS) on the Geotail spacecraft and the Comprehensive Energetic Particle and Pitch Angle Distribution (CEPPAD) Imaging Proton Sensor (IPS) from the Polar spacecraft. Table 1 provides a list of the EPIC/ICS ion energy channels. Energy channels for the CEPPAD/IPS instrument are listed in Table 2. Complete sets of data from 1995 through 2004 have been processed for the IFM database from the Geotail spacecraft. 1995 is when Geotail changed its orbit from sampling the distant magnetotail to its present orbit. The Polar ion flux measurements used date from the spacecraft's launch in 1996 through 2004.

2.1.1 Region Identification

The first step in preparing the data for the IFM database generation process is to identify the phenomenological region (i.e., solar wind, magnetosheath, magnetosphere) each ion flux measurement is made in. A tool was created in IDL (Interactive Data Language) to allow for the graphical display of plasma moment data to identify boundary

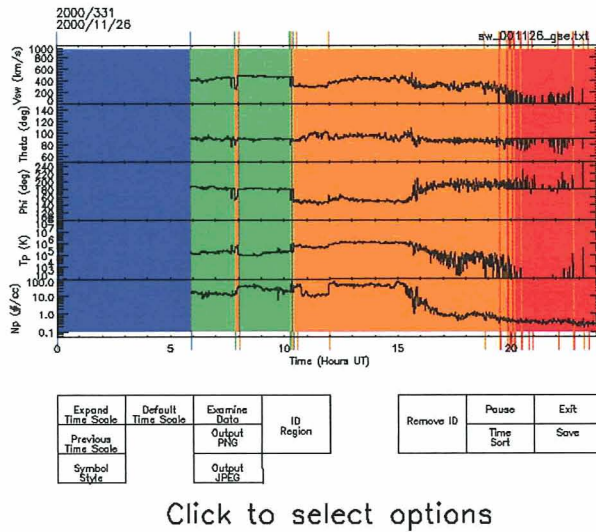


Figure 5. Graphical interface to the geospace region identification tool.

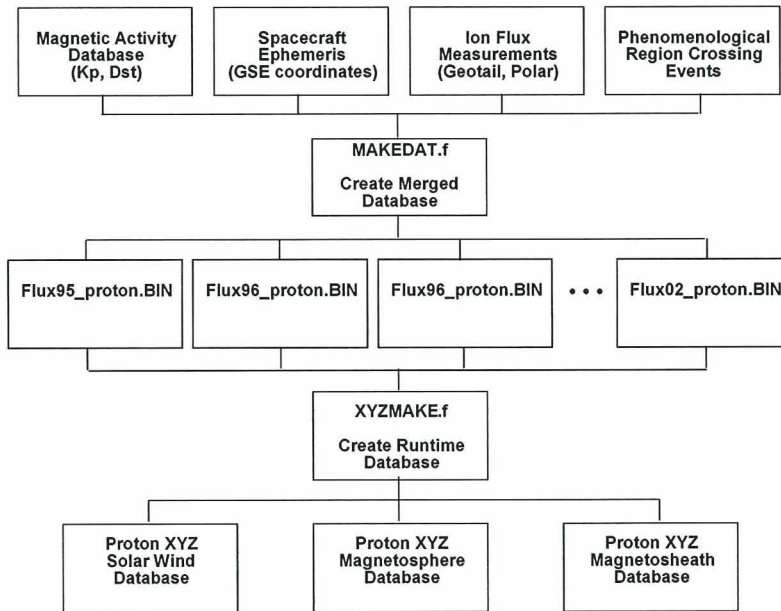


Figure 6. IFM Database Generation Process.

crossing event times (Fig. 5). A record of each region boundary crossing event was made, allowing for the association of a flux measurement with a region.

2.1.2 Database Generation

There are three steps in creating the IFM database (Fig. 6). Step 1 is the creation of merged data files for each year that data is collected. These yearly files contain information about the magnetic activity, spacecraft position, ion flux measurements, and the phenomenological region (i.e., solar wind, magnetosheath, magnetosphere). Step 2

is the creation of the runtime database files for each region. It is during this process that the flux is mapped and the statistics are compiled for elements of space whose volumes are 1 Re x 1 Re x 1 Re.

Generation of the model's database is a computationally intensive process since it requires mapping all flux values in the Polar and Geotail data sets to values in the model database. Individual databases are required for each energy, Kp value, or other input parameter, requiring significant computer resources to generate the model. However, once the databases are complete, the runtime code is computationally efficient since the time consuming calculations take place during database generation. Database generation is implemented in three steps:

Step 1: Create a database of "streamline" position points that trace out the drift path available to charged particles while conserving both the total energy and the first adiabatic invariant (the magnetic moment) as they propagate through the magnetosphere. The particle drift velocity \vec{v}_D is

$$\vec{v}_D = \vec{v}_{\nabla B} + \vec{v}_{\text{Curv}} + \vec{v}_{\text{ExB}} \quad (1)$$

where

- $\vec{v}_{\nabla B}$ = B-field gradient drift velocity
- \vec{v}_{Curv} = field curvature drift velocity
- \vec{v}_{ExB} = ExB drift velocity.

The total drift velocity of a particle in and electric field \vec{E} and magnetic field \vec{B} is [Parks, 1991]

$$\vec{v}_D = \frac{\vec{E} \times \vec{B}}{B^2} + \frac{m}{qB^4} \left(v_{\parallel} + \frac{v_{\perp}^2}{2} \right) \vec{B} \times \frac{\nabla B^2}{2} \quad (2)$$

where,

- q = electric charge of the particle
- $v_{\parallel} = v \cos\alpha$ = particle speed parallel to magnetic field line
- $v_{\perp} = v \sin\alpha$ = particle speed perpendicular to magnetic field line.

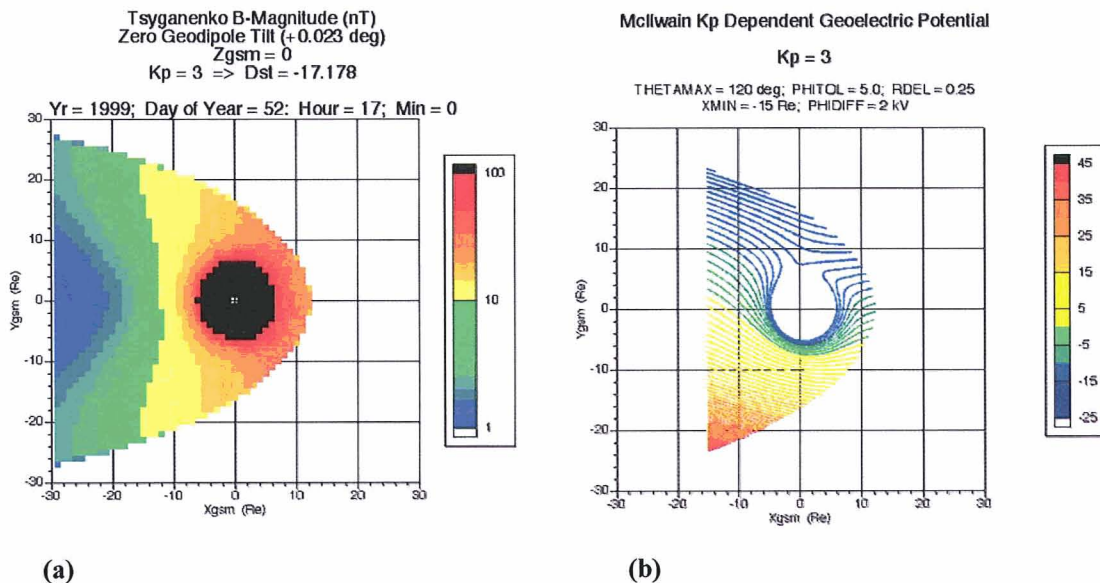


Figure 7. Magnetic and Electric Potential Models. (a) Tsyganenko magnetic field intensity $|B|$ (nT) and (b) geoelectric potential (kV) in the ZGSM = 0 plane. These values will be used to compute an example set of streamlines shown in later figures.

The Tsyganenko geomagnetic field model [Tsyganenko, 1995, 1997; Tsyganenko and Stern 1996] is used in the current version of the model since it provides magnetic field values as a function of solar wind plasma parameters and geomagnetic disturbance values. Figure 7a shows Tsyganenko total field intensity $|B|$ in the $Z_{gsm} = 0$ plane. The electric field is

$$\vec{E} = -\vec{\nabla}\Phi \quad (3)$$

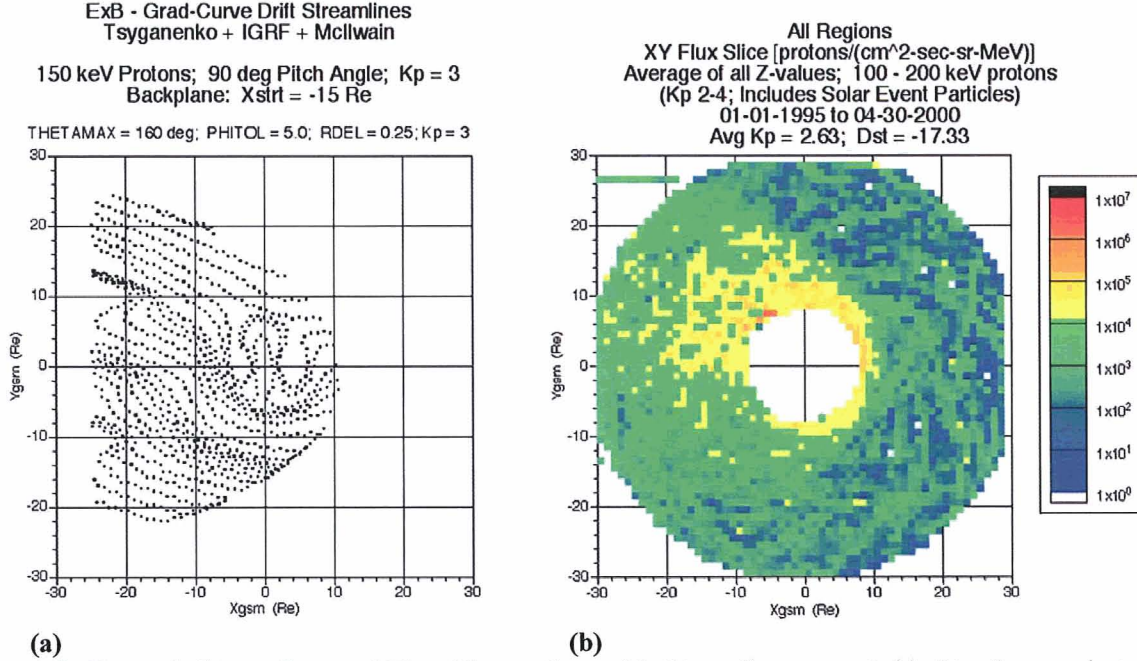


Figure 8. Example Streamlines and Flux Observations. (a) Streamlines generated in Step 2 are projected onto the $Z_{GSM} = 0$ plane and can be compared to (b) Geotail spacecraft flux data for all phenomenological regions (solar wind, magnetosheath, and magnetosphere) without streamline mapping.

where Φ is the geoelectric potential in the equatorial plane, currently provided by the McIlwain K_p -dependent model [McIlwain, 1986]. This model includes both the convective and co-rotating contributions to the electric potential. Magnetic field lines are treated as equipotential lines, allowing the potential at the equatorial plane to be mapped to higher magnetic latitudes. Figure 7b shows an example output from the McIlwain geoelectric potential model. The modeling approach used allows for the straightforward substitution of alternate geomagnetic field and geoelectric potential models if higher fidelity models are acquired or tests of particle loading into the database utilizing alternative models are desired. Higher fidelity global geoelectric field models will be evaluated for use and can be easily incorporated into the model.

The total particle energy is

$$E_{TOT} = KE_D + KE_F + PE \quad (4)$$

where,

- KE_D = kinetic energy due to particle drift
(gradient, curvature, ExB)
- KE_F = kinetic energy from particle's spiral
motion about the \vec{B} field line
- PE = particle's potential energy.

Alternatively, the energy equation (4) can be expressed in terms of the magnetic moment and geoelectric potential as

$$E_{TOT} = \frac{1}{2} m(v_D^2 + v_{\parallel}^2) + \mu B + q\Phi \quad (5)$$

with the magnetic moment given by

$$\mu = \frac{\frac{1}{2} m v_{\perp}^2}{B} \quad (6)$$

The streamlines are created by initializing the start positions of an autonomous agent (AA) algorithm representing test particles. Streamlines are found by minimizing deviations in energy and magnetic moment in the AA algorithm along the particle drift trajectory. The AA actions are based upon the calculated environments for the magnetic and electric fields for a range of activity levels, conserving particle magnetic moment and energy at each step in the calculation. Figure 8a shows an example of streamlines created for the electric and magnetic. The density of streamlines used in the actual database generation process is much higher than shown in the figure, which used a smaller number of streamlines for clarity. The streamlines in this case compare favorably to the flux distributions in the data sets as shown in Figure 8b where EPIC/IPS proton flux in the 100-200 keV energy range (for $2 \leq K_p \leq 4$) is projected onto the equatorial plane. An example of the streamlines compared to satellite measurements of magnetospheric ion flux are shown in Fig. 9, demonstrating that the streamline contours generated analytically are in good agreement with the spacecraft flux measurement data (ignore the streamline artifacts in the data “hole”).

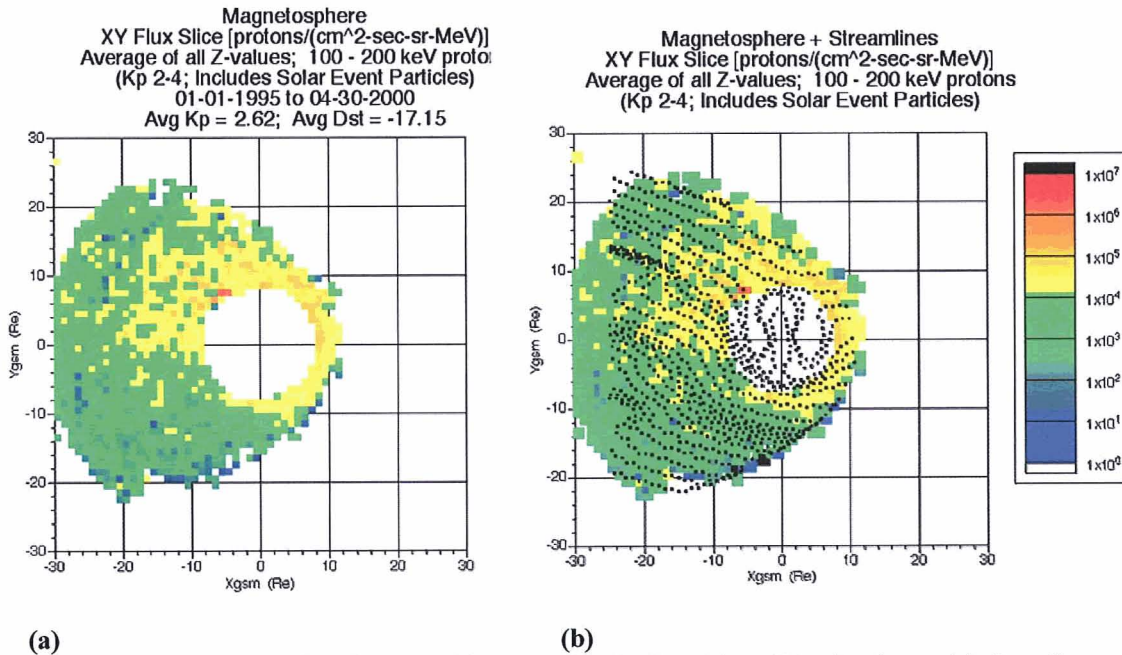


Figure 9. Streamline Overlay on Magnetospheric Ion Flux Distributions. (a) Ion flux within the magnetosphere are projected onto the $Z_{gsm} = 0$ plane. (b) Streamlines shown in Figure 2a are plotted over the ion flux distribution.

Step 2: Create a database of pointers that allow for the rapid mapping of a satellite particle flux measurement to a streamline. This cross-referencing database divides the magnetosphere into spatial volume elements that are at a much finer resolution than used in the final, runtime database used to perform flux calculations.

Step 3: Generate the runtime database, using spacecraft (Geotail, Polar) particle flux measurements. Use the region crossing database to associate each spacecraft measurement with a phenomenological region (solar wind,

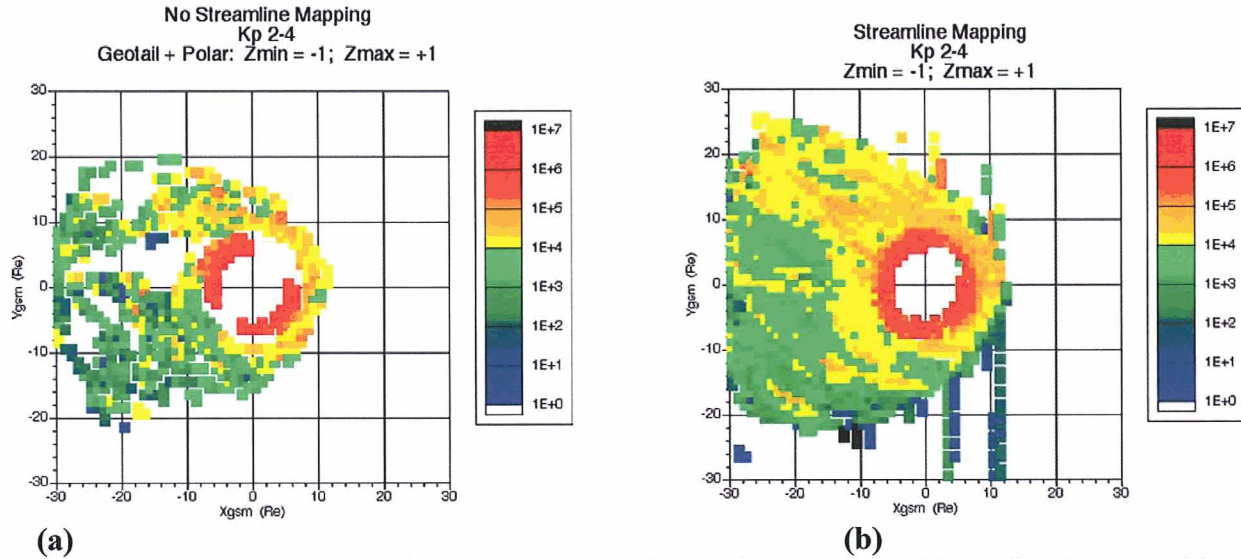


Figure 10. Magnetospheric Ion Flux Derived from Streamline Mapping. (a) Ion flux data set without mapping projected onto the GSE $Z=0$ plane and (b) the same data used with the streamline mapping algorithm.

magnetosheath, magnetosphere). Use the cross-referencing database to determine which streamline(s) to attach a given satellite measurement of magnetospheric flux to. Bin the data, based upon the magnetic activity index (e.g., K_p). Allow the flux to be mapped up and down the streamline for a relatively small distance, performing range-weighted averaging of the particle flux.

From *Roderer* [1970] we get the expression for the omnidirectional flux at a point P, expressed as an integral over the equatorial flux:

$$J(B_p) = 4\pi \frac{B_p}{B_o} \int_{\sqrt{1-\frac{B_o}{B_p}}}^{\sqrt{1-\frac{B_o}{B_E}}} \frac{j_o(\cos \alpha_o) \cos \alpha_o d(\cos \alpha_o)}{\left[1 - \frac{B_o}{B_p} (1 - \cos^2 \alpha_o)\right]} \quad (7)$$

where

- α = particle pitch angle,
- J_p = omnidirectional flux at the point P
- j_o = directional equatorial flux
- B_p = magnetic field at the point in question
- B_o = magnetic field at the field line intersection with the equatorial plane
- B_E = magnetic field at the field line intersection with the absorbing atmosphere.

Use of equation (7) allows flux to be mapped along the geomagnetic field lines from the streamline point in the equatorial plane. Accumulation of flux values in volume elements from multiple streamlines produces a position dependent database that is used to compute the ion flux statistics within each volume element. Range weighting ensures that the average flux calculated for a given volume element will reflect those measurements closest to the

volume element. Figure 10 shows that the mapping takes a sparsely populated database and more fully populates the magnetosphere database, while maintaining the overall structure.

Examples of output from the database generation process are shown in Figures 2 through 4. These flux maps show the proton flux as a function of the Kp magnetic activity index intervals. These are scatter plots of the data in the x-y plane, showing the average of all z-values. The data clearly orders up by Kp, especially in low energy plots (Fig. 2). These plots also demonstrate the sparseness of the data as Kp increases. As the energy increases, the flux decreases and the distinction between the solar wind, magnetosheath, and magnetosphere regions becomes less. As expected, the higher energy particles have free access to the magnetospheric regions modeled.

2.1.3 High Energy Ion Analysis

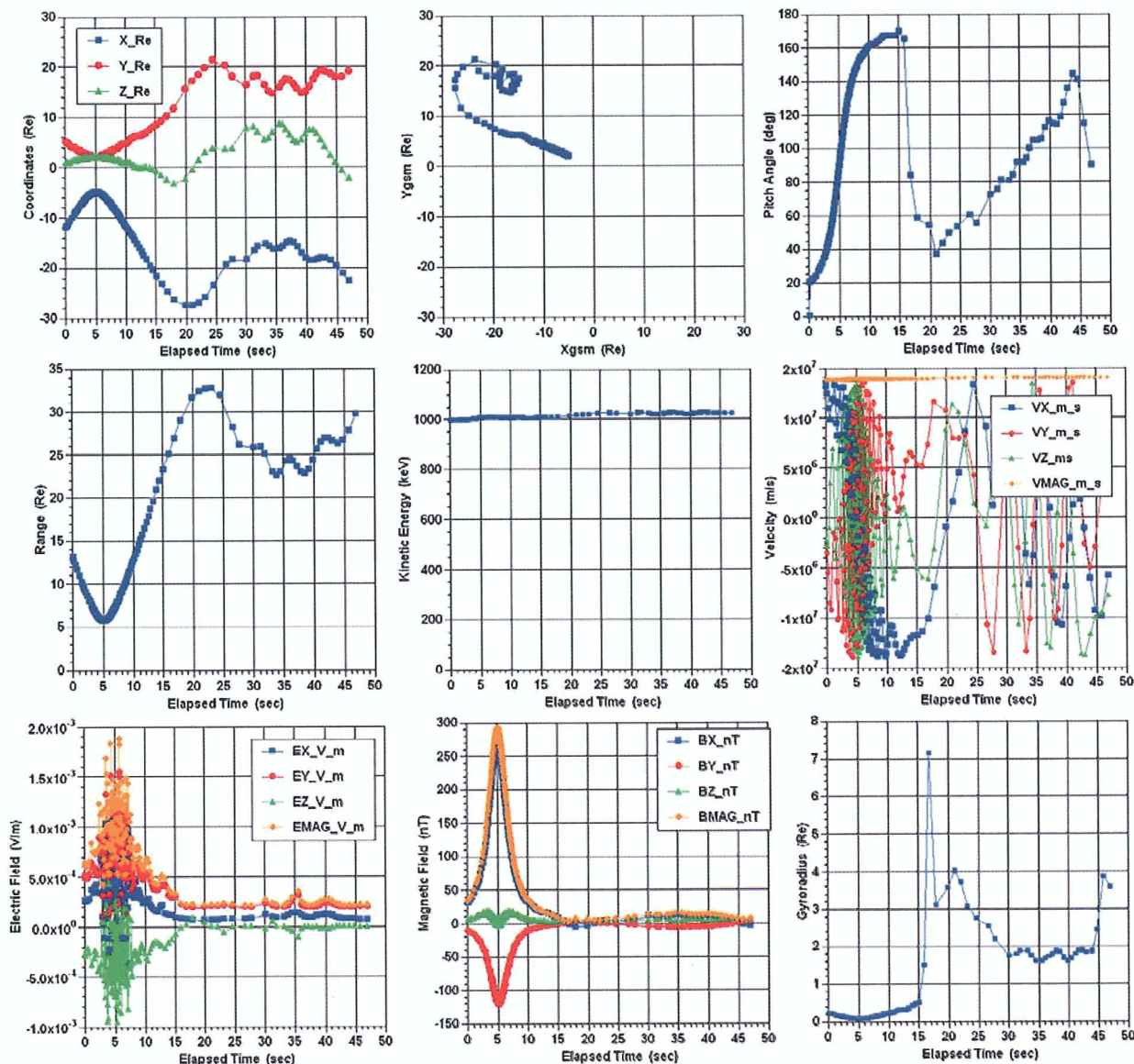


Figure 11. Diagnostic output from high energy ion Lorentz force propagator. Starting conditions for this test case: Xgsm = -12 Re; Ygsm = +5 Re; Zgsm = +1 Re; Kp = 3.0; KE = 1 MeV; Pitch Angle = +20 deg.

The streamline mapping algorithm described above has been successfully used in generating the databases for CRM. However, the guiding center approximation used for CRM will not work in cases of high kinetic energy,

where the particle's gyroradius has the possibility of exceeding the magnetic field's gradient scale length. It is for this reason that a test module was created which uses a full physics based approach that can handle non-adiabatic particle motion. The major components of the high energy ion module are: the Tsyganenko geomagnetic field model, the McIlwain geoelectric potential model, and a Lorentz force particle mover. There are three different implementations of the particle mover's integration scheme: Euler's method, Runge-Kutta with adaptive step-size, and Bulirsch-Stoer with adaptive step-size. Test cases were exercised with all three integrators. Euler's method is the simplest, but results indicated it lacked the accuracy required to propagate ions in the outer magnetosphere. Both the Runge-Kutta and Bulirsch-Stoer integrators performed well.

Figure 11 shows diagnostic output from one of the test cases using the Runge-Kutta integrator. From the range versus elapsed time calculations, it is seen that the 1 MeV particle starting at the dusk side of the outer magnetosphere with a 20 degree pitch angle mirrors after about 5 seconds at a geocentric distance of about 5 Re. The particle then heads in the tailward direction where the motion becomes chaotic once it crosses into the neutral sheet region, where the gyroradius of the particle greatly increases. However, from this and other numerical experiments it was demonstrated that the gyroradius remained relatively small except for cases where the particle entered the neutral sheet region. This and other test results suggested that the streamline methodology described earlier can be used for the energy range of particles included in the IFM database (58.1 to 1560 keV).

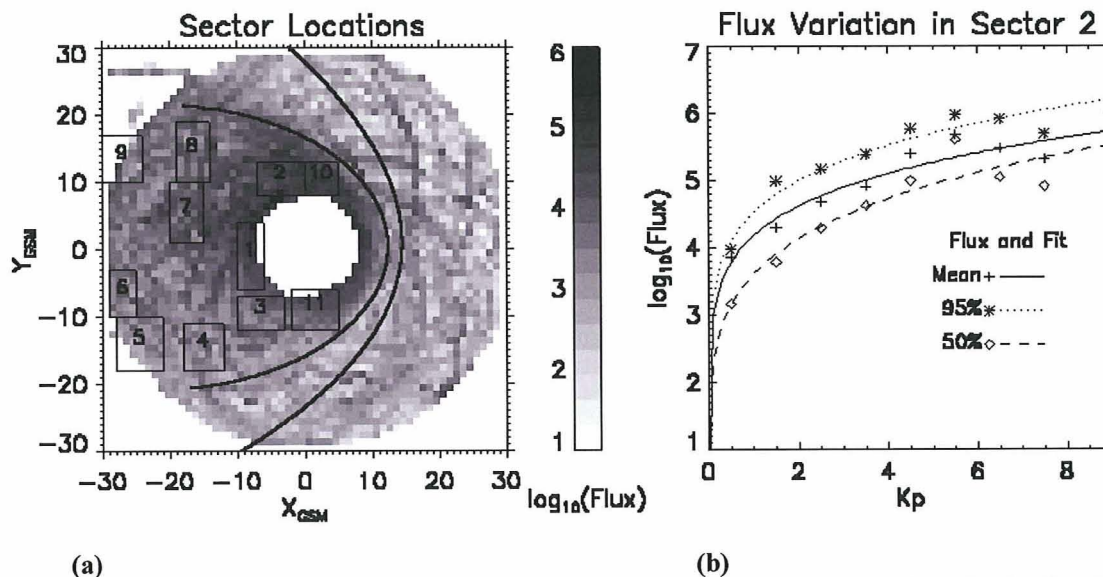


Figure 12. Flux Scaling. Sectors are identified in (a) that were used to obtain scaling laws for the flux (in units of protons/[cm²-sec-sr-MeV]) as a function of Kp. The flux variation as a function of Kp is given in (b) for Sector 2. Statistics of the flux variation for each Kp level is determined to provide a basis for estimating the probability of encountering extreme flux values and a method of scaling statistically significant scaling flux distributions at low Kp to the poor statistics in the high Kp cases (from *Blackwell et al.*, 2000a).

2.1.4 Flux Scaling

Flux measurements are sparse at large Kp ($Kp > 6$) over much of the magnetosphere. For this reason a “flux scaling” approach has been adapted from CRM [*Blackwell et al.*, 2000]. Scaling laws are used to scale the average flux for a given Kp to the mean, 50%, and 95% levels for any Kp value. Figure 12(a) shows that a number of spatial sectors were chosen so that Kp scaling laws could be derived which cover the entire range of Kp values. Figure 12(b) shows an example sector's results. Unique scaling laws are derived for each sector.

2.1.5 Polar Spacecraft Data

IFM's output energy bins are tied to the Geotail energy bins (Table 1). The number and energy limits of data channels from the Polar spacecraft (Table 2) differ from Geotail's, so the database generation software was modified so that ion flux from Polar is calculated for the Geotail energy channels. This is performed by performing a power-law fit to the spectrum for each Polar flux measurement (Fig. 13). The power-law representation of Polar data allows for the integration of the flux inside each of the Geotail energy bins.

For each point in the Polar data the power law fit of the flux is calculated over all the energy bands.

$$\text{Flux} = AE^B, \tag{8}$$

where E is the energy, $A = e^a$, and $B = b$. The least squares fitting coefficients are defined as

$$b = \frac{n \sum (\ln x_i \ln y_i) - \sum (\ln x_i) \sum (\ln y_i)}{n \sum (\ln x_i)^2 - (\sum \ln x_i)^2} \tag{9}$$

$$a = \frac{\sum (\ln y_i) - b \sum (\ln x_i)}{n} \tag{10}$$

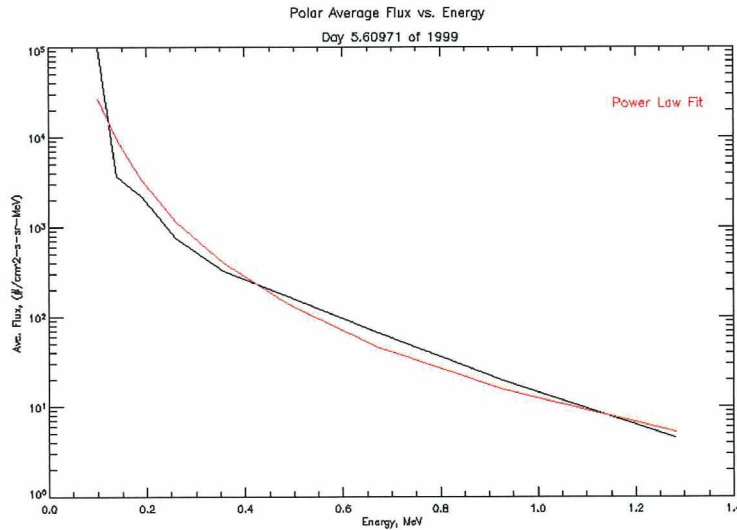


Figure 13. Power-law fit to a Polar spacecraft flux measurement.

where x is the energy and y is the flux. The flux for Polar in the Geotail energy band was determined from the power law fit.

$$\text{Flux} = \frac{A (E_2^{(B+1)} - E_1^{(B+1)})}{(B+1)(E_2 - E_1)} \tag{11}$$

where E2 and E1 are the upper and lower bounds of the energy band, respectively. A and B are defined above.

III. Runtime Model

The runtime code for CRM and IFM share a great deal in common in their overall structure (Fig. 14). However, significant modifications were made so that IFM can handle not just one, but multiple energy bands in calculating

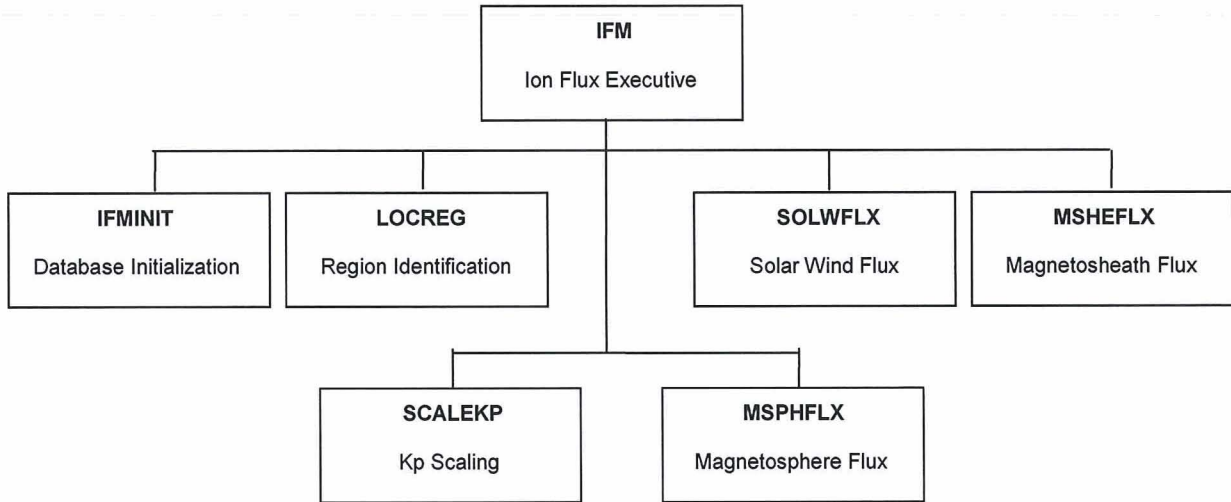


Figure 14. Major software modules in IFM.

flux. Figures 15 – 17 are examples of output from IFM. These are scatter plots of the proton flux predicted by IFM in the $Z_{gsm} = 0$ plane for a range of Kp geomagnetic activity indices. Figure 18 shows the mission fluence calculated for each of the energy channels available in IFM, using the Chandra ephemeris as an example. These plots show the utility of mapping the data, since the code fills in large spatial gaps between flux values, while still maintaining the overall spatial distribution of the flux. The user can control the extent of the near-neighbors used in calculating flux at a point. Also available to the user are a variety of smoothing algorithms.

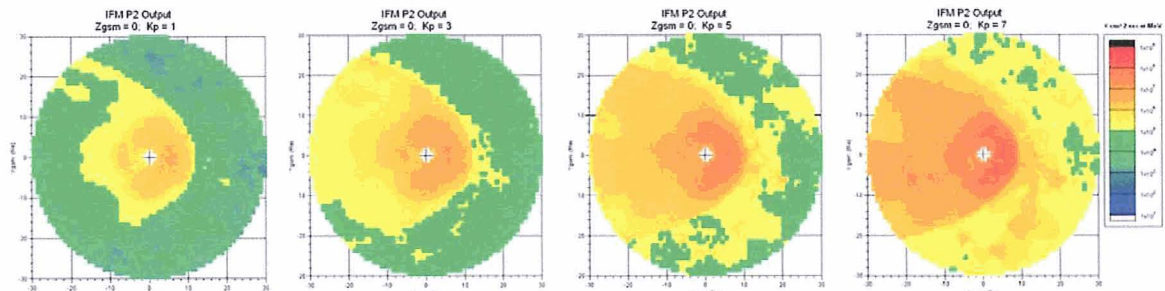


Figure 15. Kp variation for P2 channel with spatial sector weighting.

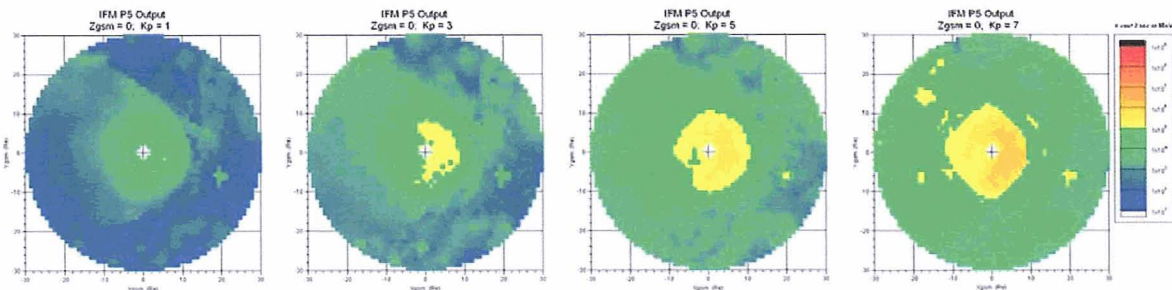


Figure 16. Kp variation for P5 channel with spatial sector weighting.

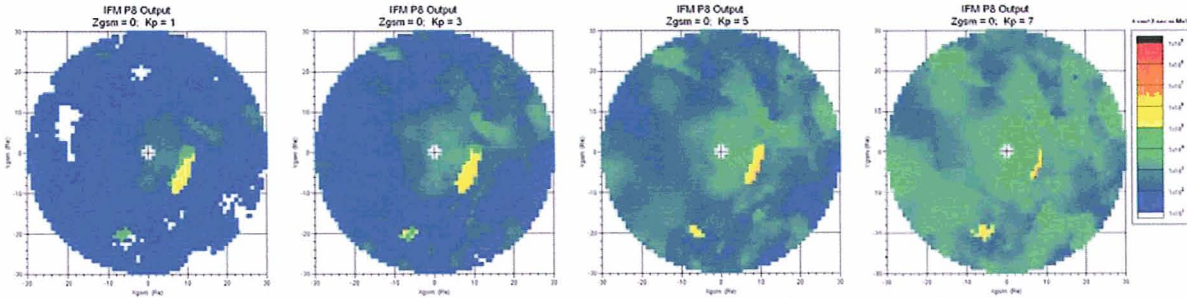


Figure 17. Kp variation for P8 channel with spatial sector weighting.

The user must decide whether to use the Kp-correlated database included with IFM v1.0 or to use a Kp + ACE-correlated database (not yet available).

III. Summary

IFM is a radiation environment risk mitigation tool that provides magnetospheric ion flux values for varying geomagnetic disturbance levels in the geospace environment. IFM incorporates ion flux observations from the Polar and Geotail spacecraft in a single statistical flux model. IFM is an engineering environment model developed to predict the proton flux in the solar wind, magnetosheath, and magnetosphere phenomenological regions of geospace. The development of IFM has heavily leveraged experience gained in creating the ion flux model for the Chandra X-ray observatory. This database allows for IFM output to be correlated with the geomagnetic activity level, as represented by the Kp index.

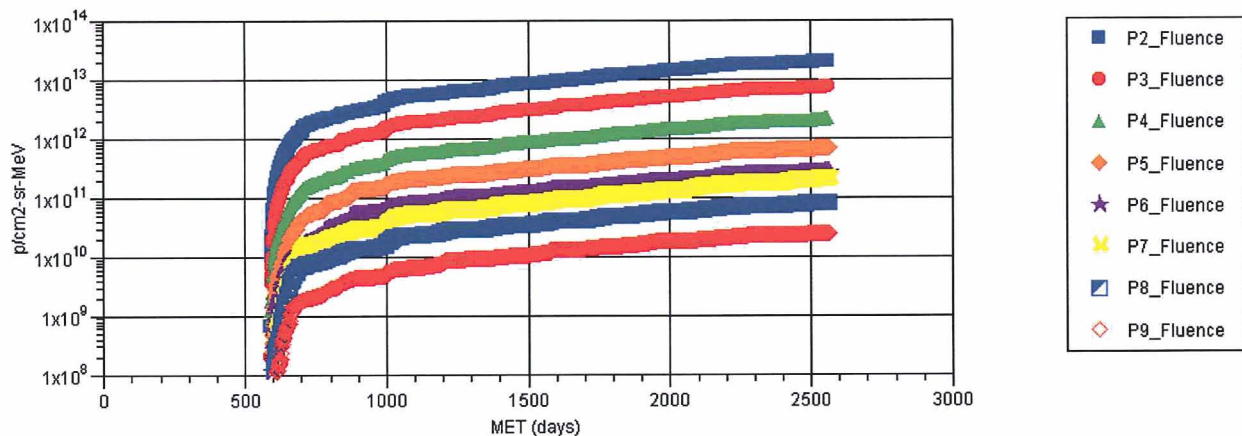


Figure 18. IFM fluence (#/cm²-sr-MeV) for Chandra ephemeris.

Acknowledgements

Geotail EPIC/IPS data was provided by Dr. Richard McEntire and Mr. Stuart Nylund (JHU/APL). Polar CEPPAD/IPS data was provided by Dr. Harlan Spence, Boston University. Geomagnetic indices were obtained from the NOAA National Geophysical Data Center. Geotail CPI/Hot Plasma Analyzer data plots were provided courtesy of Dr. Louis Frank and Dr. William R. Patterson, University of Iowa. WCB and AMD were supported by NASA Contract NNM05AB50C to Jacobs Engineering.

References

- Bennett, L., M. G. Kivelson, K.K. Khurana, L. A. Frank, and W. R. Patterson, A model of the Earth's distant bow shock, *J.Geophys.Res.*, 102, 26927, 1997.
- Blackwell, W.C., J. I. Minow, S.L. O'Dell, R.M. Suggs, D.A. Swartz, A.F. Tennant, S.N. Virani, & K.M. Warren, "Modeling the Chandra space environment", in *X-Ray and Gamma-Ray Instrumentation for Astronomy XI, Proc. SPIE*, **4140**, pp. 111 – 122, 2000.
- Blackwell, W.C., J. I. Minow, S. Smith, W.R. Swift, S.L. O'Dell, and R. Cameron, The Chandra X-ray Observatory Radiation Environment Model, AIAA-2003-1228, 2003.
- McIlwain, C.E., "A Kp dependent equatorial electric field model," *Advances in Space Research*, 6, 187 – 197, 1986.
- Roederer, J.G., *Dynamics of Geomagnetically Trapped Radiation*, Springer-Verlag, New York, NY, 1970.
- Sawyer, D.W., and J.I. Vette, "AP-8 Trapped Proton Environment for Solar Maximum and Solar Minimum," National Space Science Data Center, NASA Goddard Space Flight Center, NSSDC/WDC-A-R&S 76-06, 1976.
- Teague, M.J., and J.I. Vette, "A model of the trapped electron population for solar minimum," National Space Science Data Center, NASA Goddard Space Flight Center, NSSDC 03-74, 1974.
- Tsyganenko, N.A. Modeling the Earth's magnetospheric magnetic field confined within a realistic magnetopause, *J. Geophys.Res.*, 100, 5599, 1995.
- Tsyganenko, N.A., and D.P. Stern, Modeling the global magnetic field of the large-scale Birkeland current systems, *J.Geophys.Res.*, 101, 27187, 1996.
- Tsyganenko, N.A., An empirical model of the substorm current wedge, *J.Geophys.Res.*, 102, 19935, 1997.
- Vette, J.I., "The AE-8 trapped electron model environment," National Space Science Data Center, NASA Goddard Space Flight Center, NSSDC/WDC-A-R&S 91-24, 1991.

AIAA-2007-1099

The Empirical Low Energy Ion Flux Model for the Terrestrial Magnetosphere



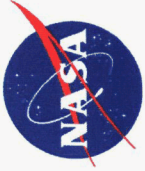
William C. Blackwell
Jacobs Engineering, MSFC Group
NASA, Marshall Space Flight Center

Joseph I. Minow
EV13/Natural Environments Branch
NASA, Marshall Space Flight Center

Anne M. Diekmann
Jacobs Engineering, MSFC Group
NASA, Marshall Space Flight Center

*45th AIAA Aerospace Sciences Meeting
Reno, Nevada 8-11 January 2007*





Acknowledgements

- NASAMSFC
 - Rob Suggs
- Sverdrup Team
 - Them Bui
 - Wesley Swift
- Johns Hopkins / Applied Physics Laboratory
 - Richard McIntire
 - Stuart Nylund
- Boston University
 - Harlan Spence
- This work performed on NASA Contract NNM05AB50C to Jacobs Engineering.

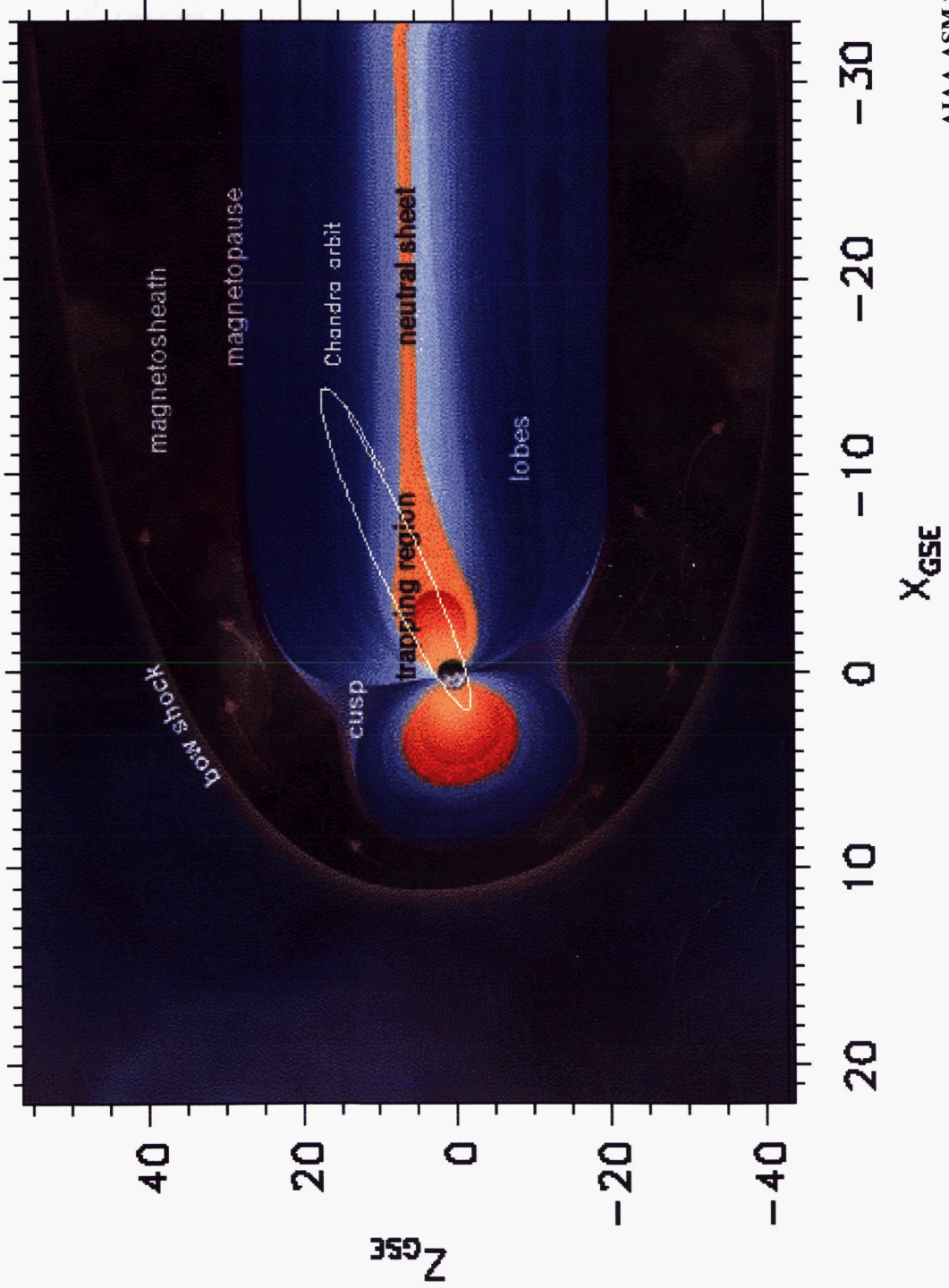


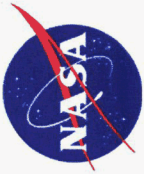
Overview

- Introduction
- Technical Approach
- Model Implementation
 - Region Identification
 - Database Generation
 - High Energy Ion Analysis
 - Flux Scaling
 - Polar Spacecraft Data
- Runtime Model
- Summary



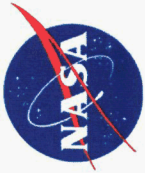
Geospace Plasma Regimes





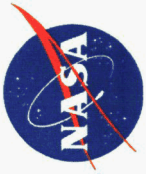
IFM Version 1 Features

- **The Living With a Star Ion Flux Model (IFM) is a radiation environment risk mitigation tool**
- **Database in GSM coordinate system**
 - Magnetotail aligned system
 - Provides seasonal, time of day variations
- **XYZ volumetric data bins used**
 - Average flux calculated for each bin
- **Nearest-neighbor approach used to get S/C's flux along ephemeris**
 - Cannot interpolate across phenomenological regions
 - (solar wind, magnetosheath, magnetosphere)
 - Constraints placed on near-neighbor choice
 - Use Z_{GSM} layers



IFM Version 1 Features (cont'd)

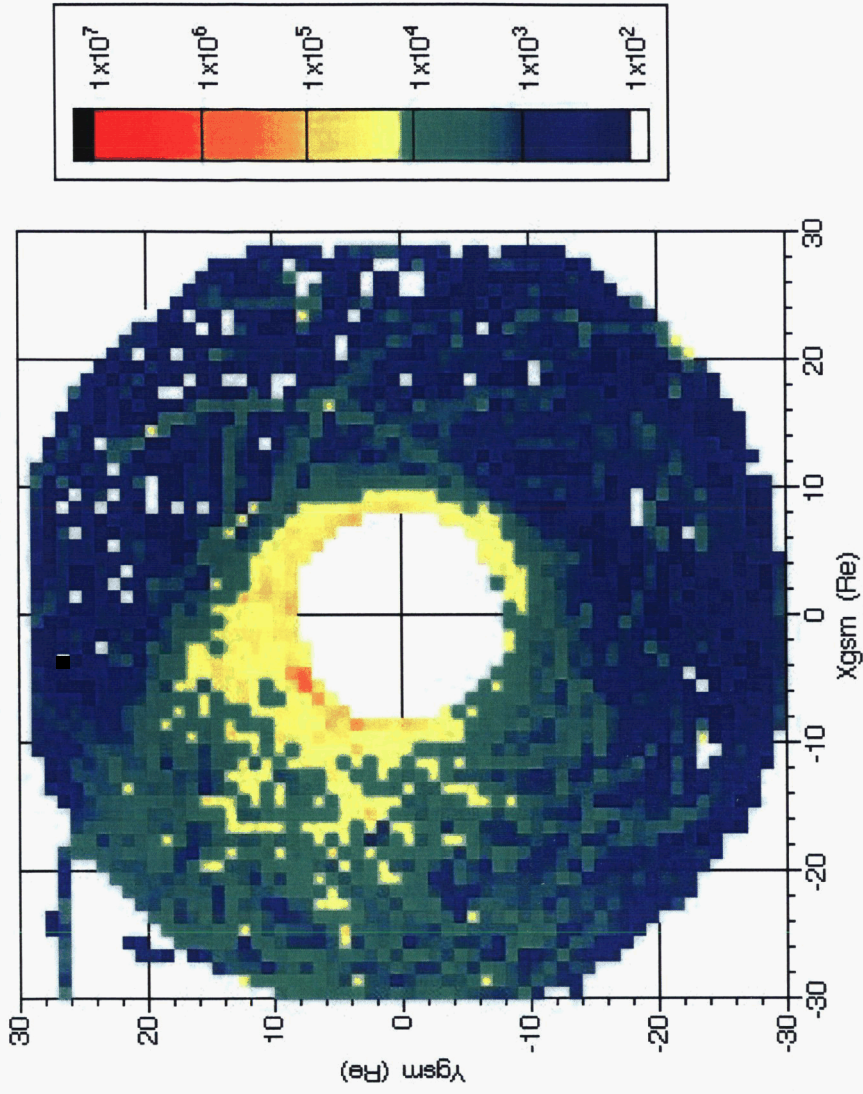
- **Polar proton flux database**
 - Years: 1997 - 2004
 - Data maps to higher magnetic latitudes
- **Geotail proton flux database**
 - Years: 1995 – 2004
 - Near equatorial orbit (8 x 30 Re)
- **Streamline/fieldline mapping of data**
 - ExB and gradient-curvature particle drift
 - Fills in spatial gaps
 - Provides predictions at high magnetic latitudes

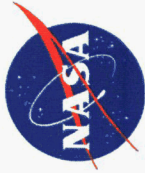


Data Overview: X-Y Plane

- 100-200 keV protons
- Gradient B-curvature drift drives ion flux through dusk sector
- Ion fluxes observed throughout magnetotail region

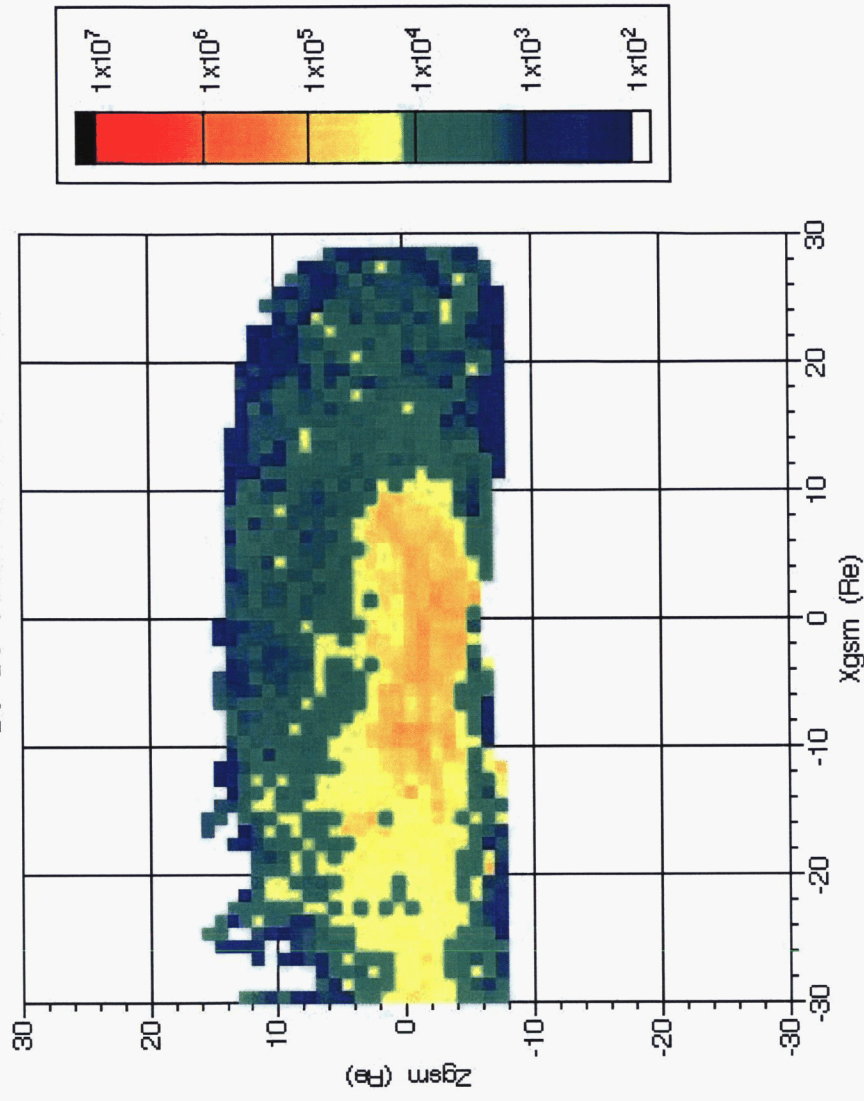
All Regions
XY Flux Slice protons/(cm²-sec-sr-MeV)
Average of all Z-values; 100 - 200 keV ions
(No Filter on Magnetic Activity; Includes Solar Event Particles)
01-01-1995 to 12-31-1999



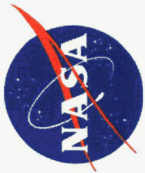


Data Overview: X-Z Plane

XZ Flux Slice [ions/(cm²-sec-sr-MeV)]
Average of all Y-values; 100 - 200 keV ions
(No Filter on Magnetic Activity; Includes Solar Event Particles)
01-01-1995 to 12-31-1999

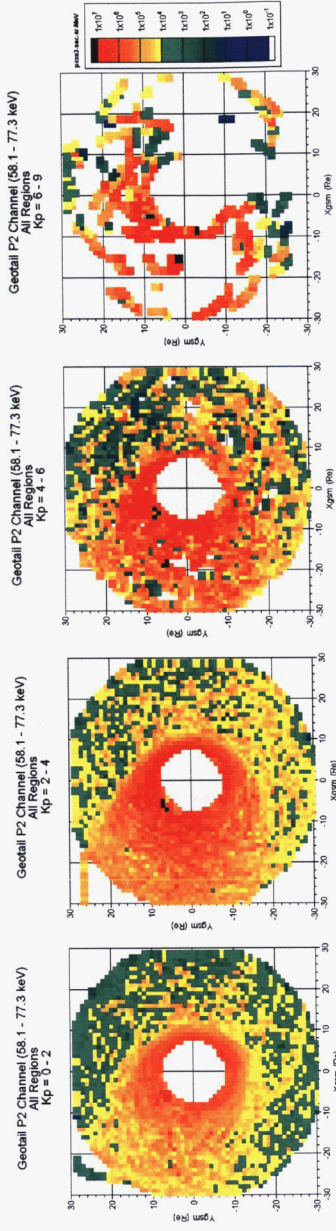


- Proton flux peaks near equatorial plane
- Abrupt decrease in flux at magnetopause on day side (X ~ 10 Re)
- Protons observed throughout magnetotail (X < -10 Re)
- Flux decreases at high latitudes

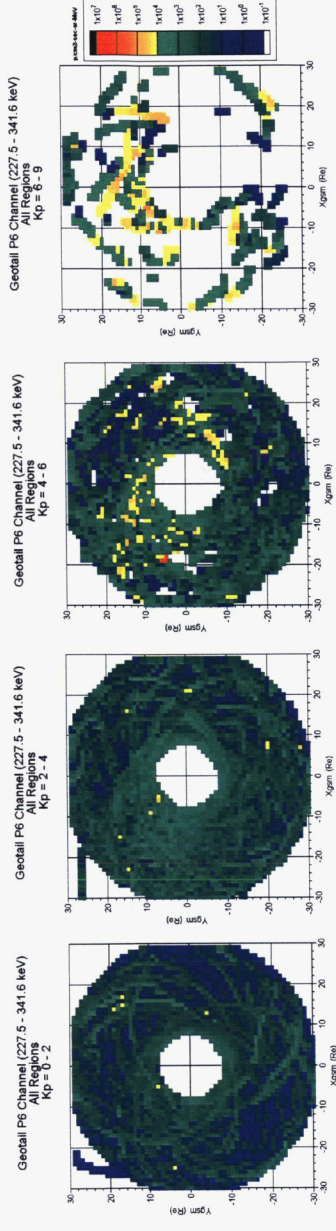


Proton Flux Correlation with Kp

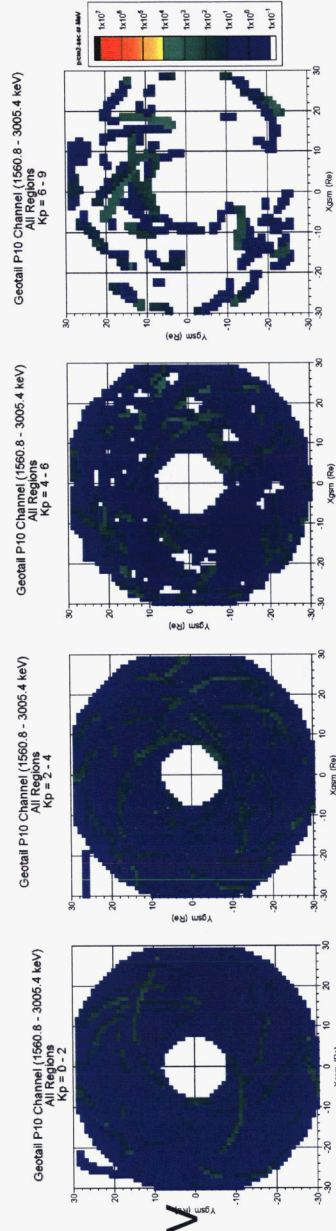
- 58.1 – 77.3 keV



- 227.5 – 341.6 keV



- 1560.8 – 3005.4 keV





Geotail EPIC/ICS Energy Bands

Channel Name	Species	Energy Band (keV/e)	Sector (deg)	Time Res. ^a (sec)	Time Res. Database ^b (sec)
P2	p+	58.1 - 77.3	22.5	6	288
P3	p+	77.3 - 107.4	22.5	48	288
P4	p+	107.4 - 154.3	22.5	48	288
P5	p+	154.3 - 227.5	22.5	48	288
P4	p+	107.4 - 154.3	22.5	48	288
P5	p+	154.3 - 227.5	22.5	48	288
P6	p+	227.5 - 341.6	22.5	48	288
P7	p+	341.6 - 522.5	22.5	48	288
P8	p+	522.5 - 813.5	22.5	48	288
P9	p+	813.5 - 1560.8	22.5	96	288
P10	p+	560.8 - 3005.4	22.5	96	288

^aTime resolution of original data.

^bTime resolution of spin averaged data obtained from Principle Investigator.

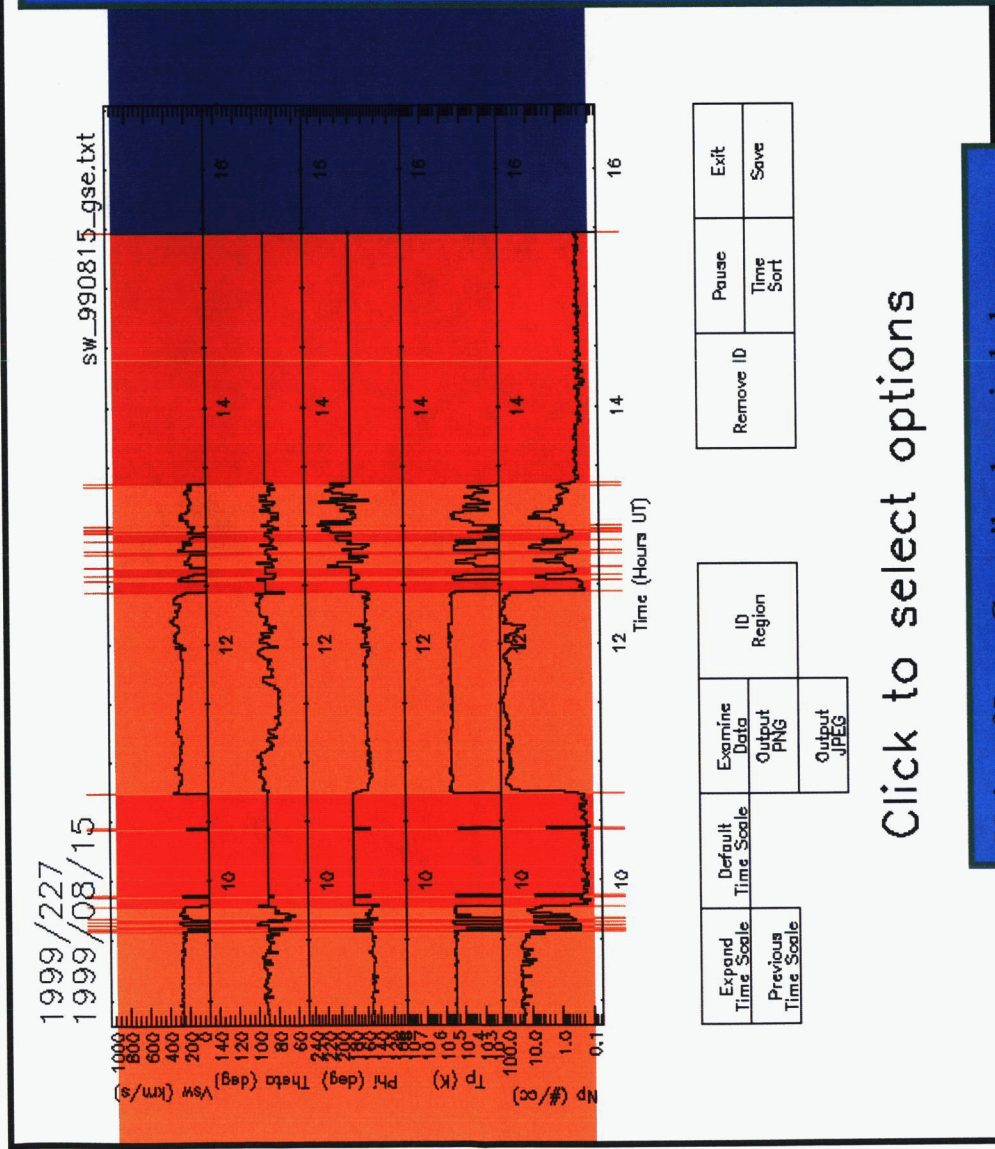


Polar CEPPAD/IPS Energy Bands

Energy Channel	Species	Energy Threshold Set 1		Energy Threshold Set 2	
		Min (keV)	Mid (keV)	Min (keV)	Mid (keV)
0	H+	16.8	18.9	13.9	15.6
1	H+	21.2	24.4	17.5	19.9
2	H+	27.9	32.4	22.6	26.2
3	H+	37.5	43.1	30.3	35.4
4	H+	49.6	57.2	41.4	48.1
5	H+	65.9	76.0	55.9	55.2
6	H+	87.7	102.0	75.9	88.4
7	H+	118.0	138.0	103.0	121.0
8	H+	161.0	188.0	142.0	168.0
9	H+	221.0	259.0	198.0	234.0
10	H+	303.0	355.0	277.0	327.0
11	H+	417.0	489.0	387.0	459.0
12	H+	574.0	674.0	543.0	643.0
13	H+	791.0	929.0	762.0	903.0
14	H+	1091.0	1281.0	1071.0	1269.0
15	H+	1505.0	2000.0	1505.0	2000.0



Plasma Regime Identification Tool

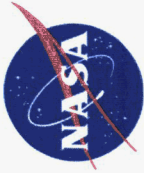


Processed: sw_990815_gse.txt

Time (UT)	ID	Region
0.00000	1	MS
9.57056	1	MS
9.58409	2	MP
9.59704	1	MS
9.62527	2	MP
9.66527	1	MS
9.69292	2	MP
9.78646	1	MS
9.86823	2	MP
9.88186	1	MS
10.4373	2	MP
10.4506	1	MS
10.7353	2	MP
12.4470	1	MS
12.5427	2	MP
12.5821	1	MS
12.6496	2	MP
12.7589	1	MS
12.7859	2	MP
12.8681	1	MS
12.9345	2	MP
12.9616	1	MS

Click to select options

Univ. of Iowa Geotail solar wind plasma moments (CPI or SWA) used for regime identifications



Flux Mapping

- **Step 1:** Create a database of “streamline” position points by computing ion test particle drift paths through the magnetosphere:

$$\vec{V}_D = \vec{V}_{VB} + \vec{V}_{Curv} + \vec{V}_{ExB} = \frac{\vec{E} \times \vec{B}}{B^2} + \frac{m}{qB^4} \left(v_{\parallel} + \frac{v_{\perp}^2}{2} \right) \vec{B} \times \frac{\nabla B^2}{2}$$

- conserving both the total energy and the first adiabatic invariant (the magnetic moment).

$$E_{tot} = \frac{1}{2} m (v_{\perp}^2 + v_{\parallel}^2) + q\phi$$

- **Step 2:** Create a pointer database that allows for rapid mapping of a satellite particle flux measurement to a streamline.
- **Step 3:** Generate runtime database using spacecraft (Geotail, Polar) particle flux measurements
 - Map flux along field lines assuming isotropic flux distribution

$$J(B_p) = 4\pi \frac{B_p}{B_o} \int_{\sqrt{1-\frac{B_o}{B_p}}}^{\sqrt{1-\frac{B_o}{B_E}}} \frac{j_o(\cos \alpha_o) \cos \alpha_o d(\cos \alpha_o)}{\left[1 - \frac{B_o}{B_p} (1 - \cos^2 \alpha_o)\right]}$$

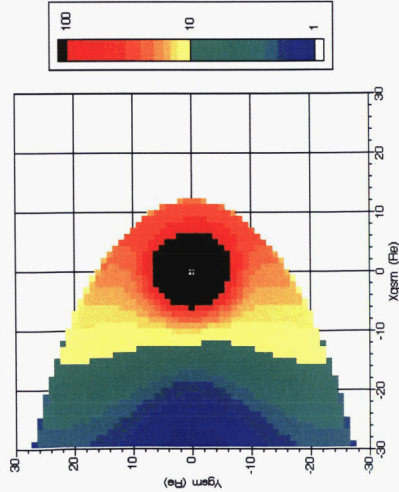


Streamline Generation

Tsyganenko B-Magnitude (mT)
Zero Geodipole Tilt (+0.023 deg)
Zgsm = 0

Kp = 3 ⇒ Dst = -17.178

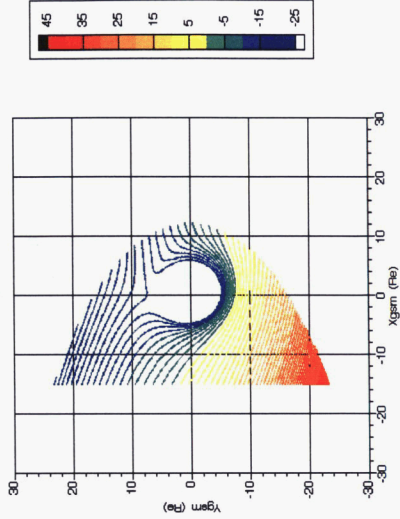
Yr = 1999, Day of Year = 52; Hour = 17; Min = 0



Mcllwain Kp Dependent Geoelectric Potential

Kp = 3

THETAMAX = 120 deg; PHITOL = 5.0; RDEL = 0.25
XMIN = -15 Re; PHIDIFF = 2 kV



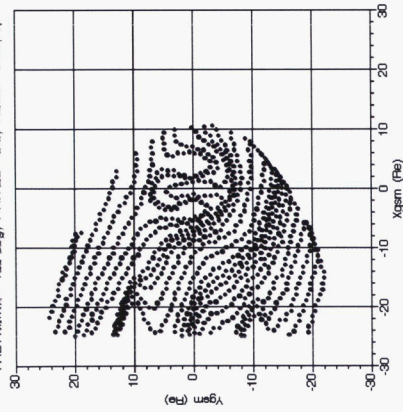
ExB - Grad-Curve Drift Streamlines

Tsyganenko + IGRF + Mcllwain

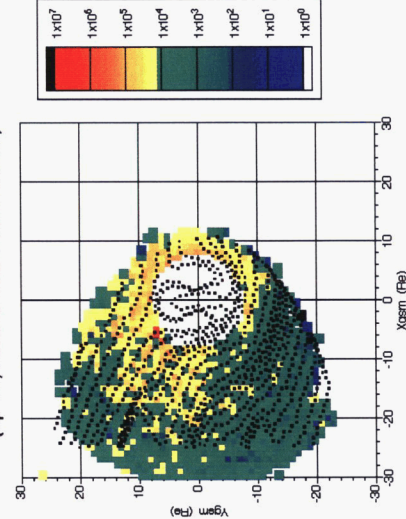
150 keV Protons; 90 deg Pitch Angle; Kp = 3

Backplane: Xsfit = -15 Re

THETAMAX = 180 deg; PHITOL = 5.0; RDEL = 0.25; Kp = 3



Magnetosphere + Streamlines
XY Flux Slice [protons/(cm²-sec-sr-MeV)]
Average of all Z-values; 100 - 200 keV protons
(Kp 2-4; includes Solar Event Particles)





Mapping

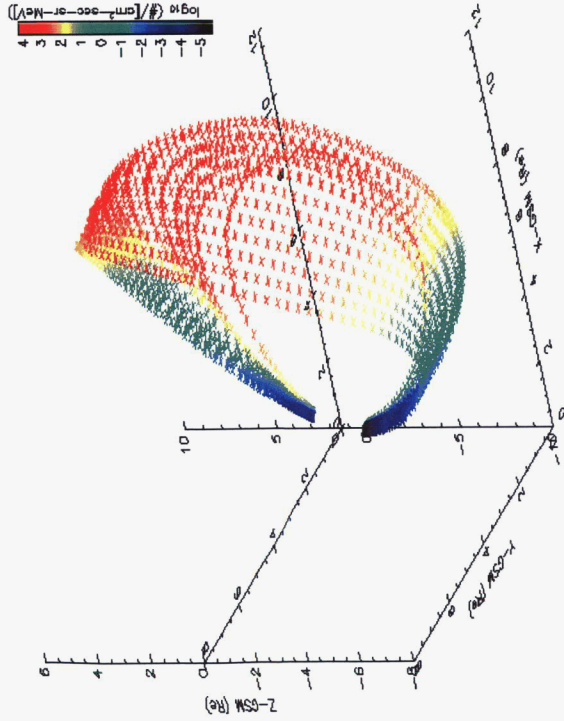
1999/200.3

$K_p = 3.5$

$Dst = -20$ nT

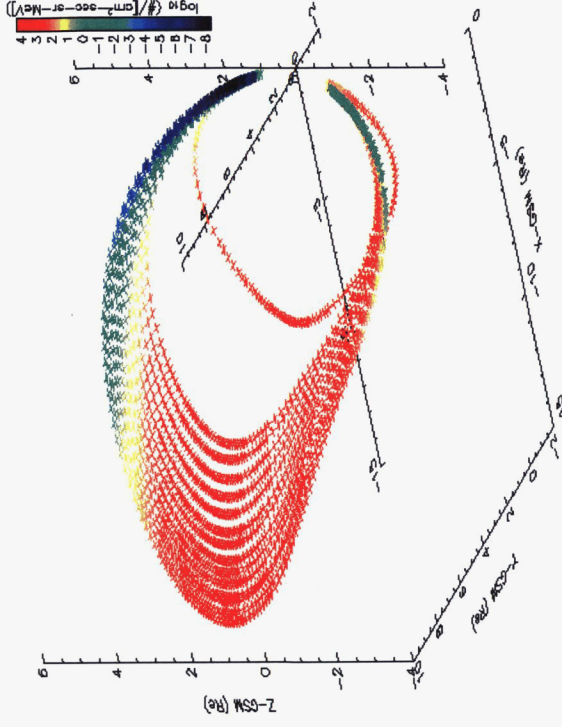
Solar wind proton flux = 1×10^4 #/cm²-sec-sr-MeV

Region = magnetosphere



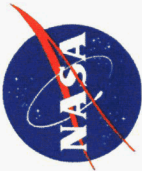
Day

• $X_{GSE} = 9 R_e, Y_{GSE} = 1 R_e, Z_{GSE} = 0 R_e$

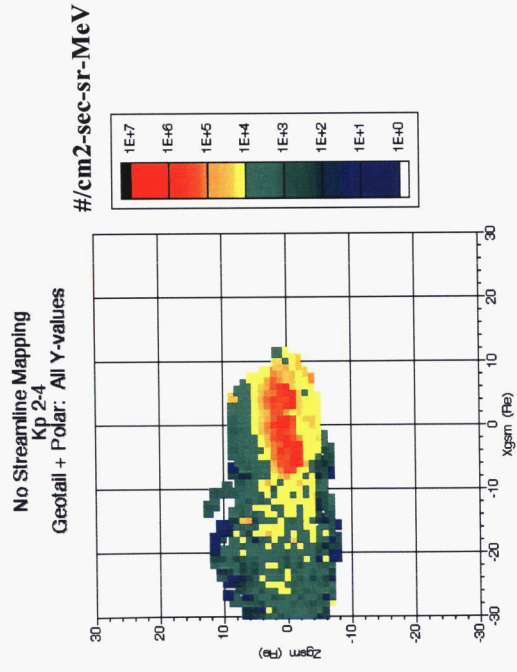
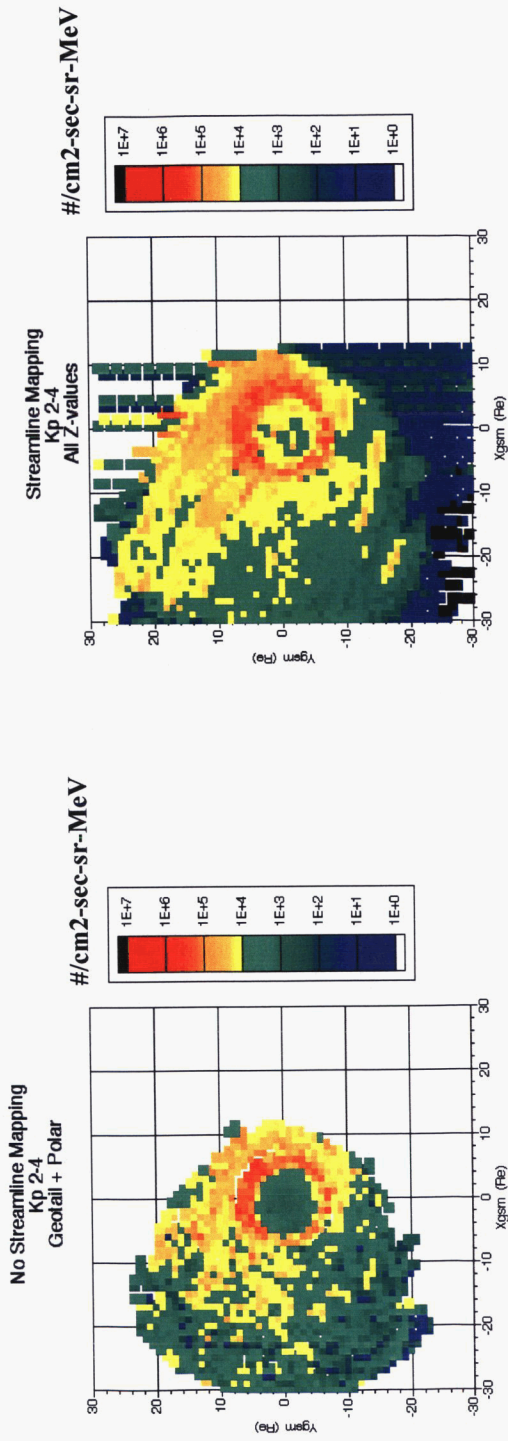


Night

• $X_{GSE} = -9 R_e, Y_{GSE} = -1 R_e, Z_{GSE} = 0 R_e$

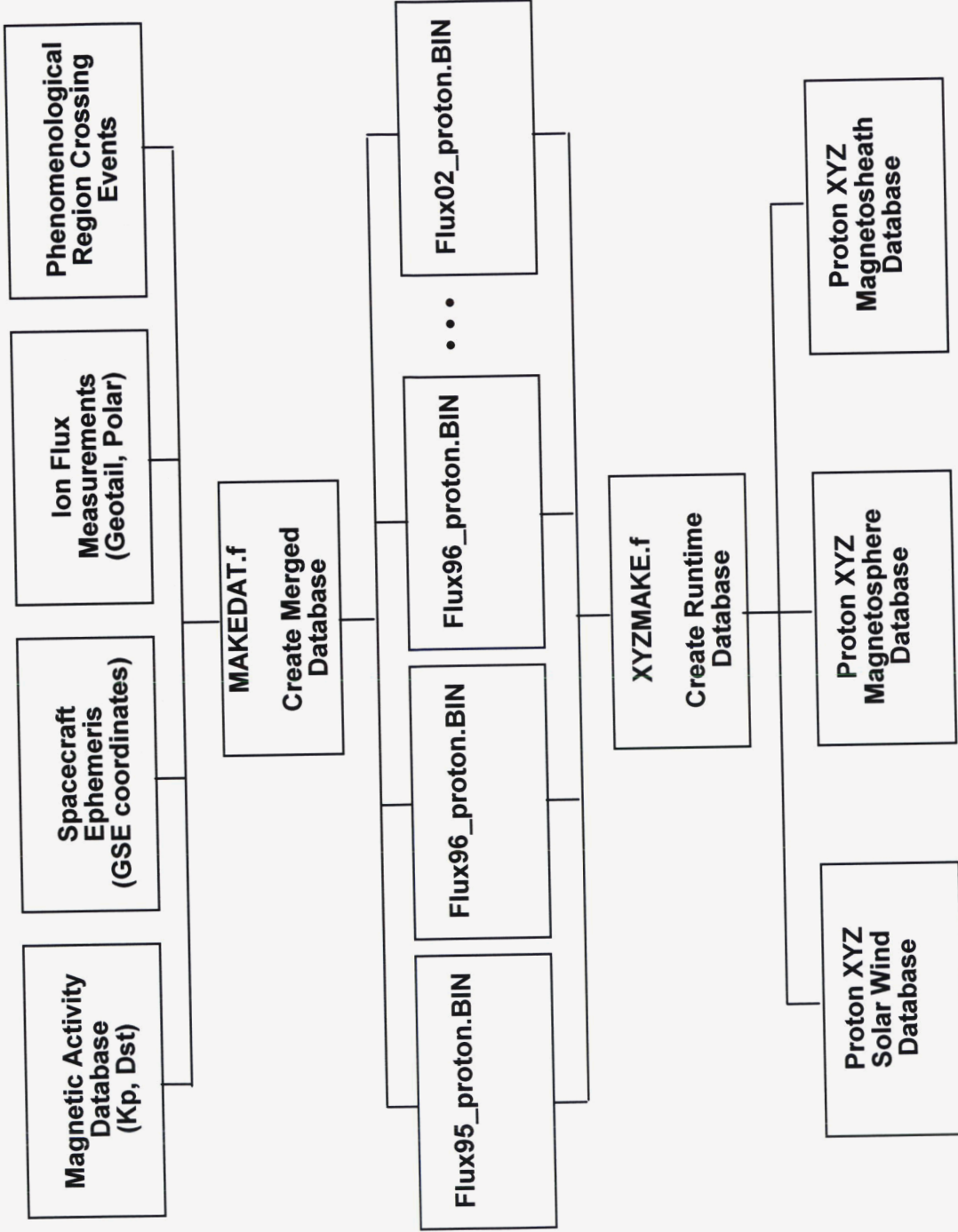


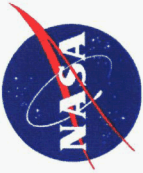
Streamline Flux Mapping



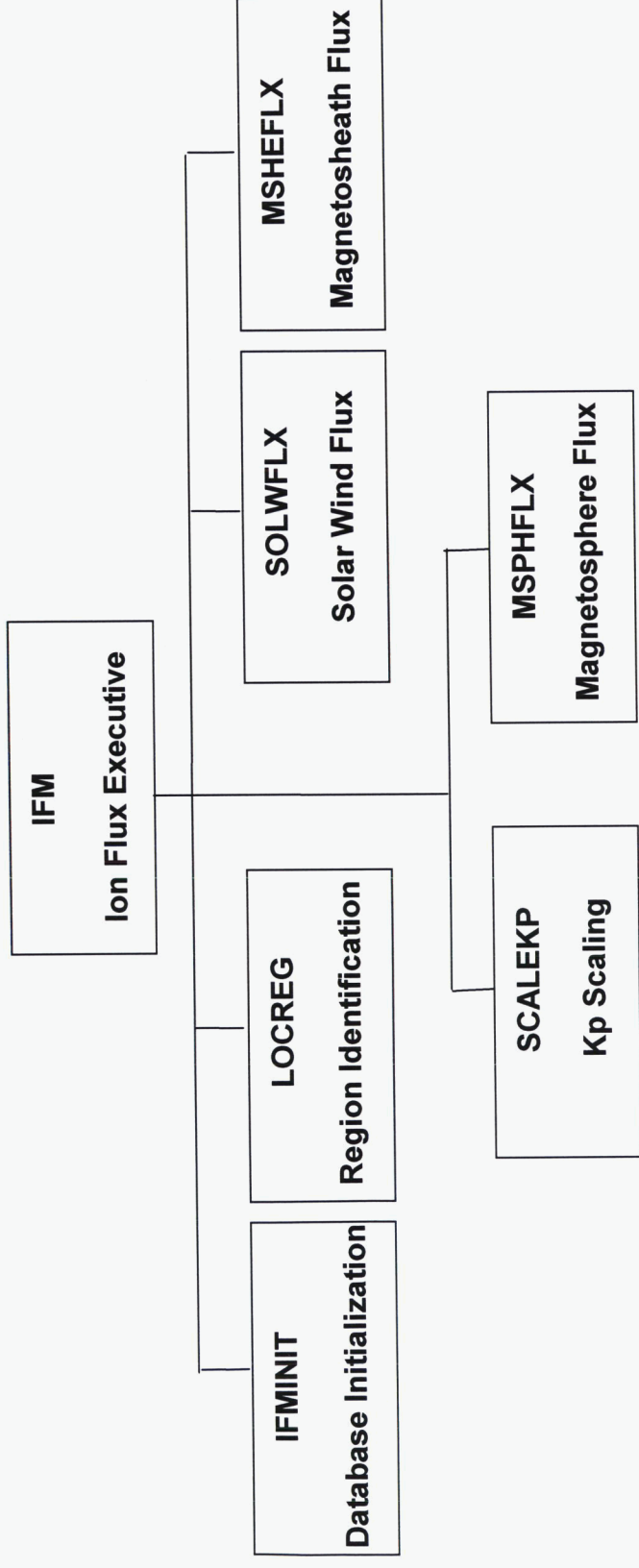


IFM Database Generation Process

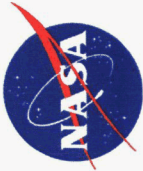




Major Software Modules in IFM

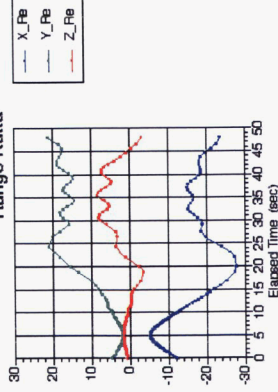


- CRM and IFM share much in common in overall code structure
- Significant modifications made so IFM can handle multiple energy bands

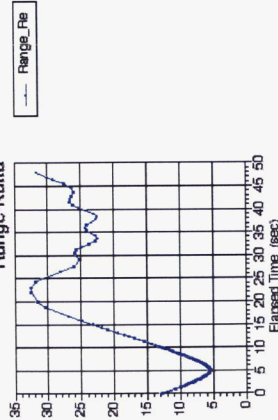


LWS IFM High Energy Ion Model Output

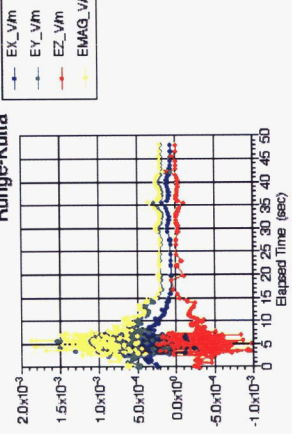
Xsirt = -12 ; Ysirt = +5 ; Zsirt = +1.
 Kp = 3.0 ; EngSirt = 1000 keV
 PAsirt = +20 deg ; AZMsirt = +30 deg
 Runge-Kutta



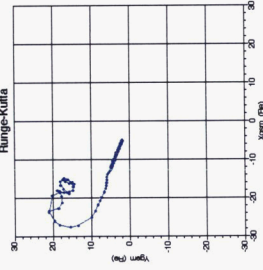
Xsirt = -12 ; Ysirt = +5 ; Zsirt = +1.
 Kp = 3.0 ; EngSirt = 1000 keV
 PAsirt = +20 deg ; AZMsirt = +30 deg
 Runge-Kutta



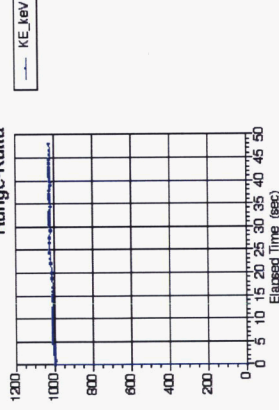
Xsirt = -12 ; Ysirt = +5 ; Zsirt = +1.
 Kp = 3.0 ; EngSirt = 1000 keV
 PAsirt = +20 deg ; AZMsirt = +30 deg
 Runge-Kutta



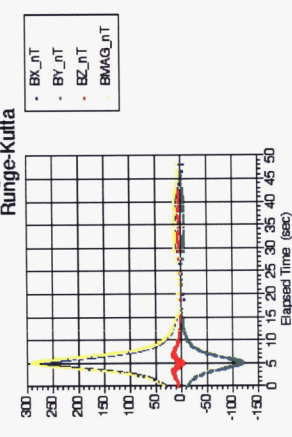
Xsirt = -12 ; Ysirt = +5 ; Zsirt = +1.
 Kp = 3.0 ; EngSirt = 1000 keV
 PAsirt = +20 deg ; AZMsirt = +30 deg
 Runge-Kutta



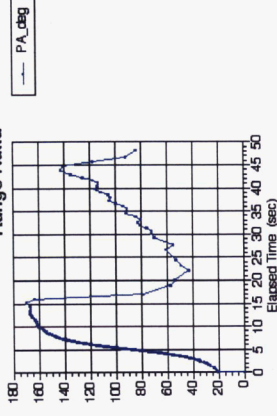
Xsirt = -12 ; Ysirt = +5 ; Zsirt = +1.
 Kp = 3.0 ; EngSirt = 1000 keV
 PAsirt = +20 deg ; AZMsirt = +30 deg
 Runge-Kutta



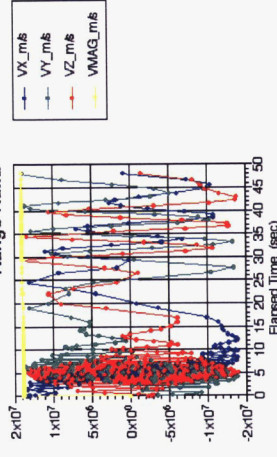
Xsirt = -12 ; Ysirt = +5 ; Zsirt = +1.
 Kp = 3.0 ; EngSirt = 1000 keV
 PAsirt = +20 deg ; AZMsirt = +30 deg
 Runge-Kutta



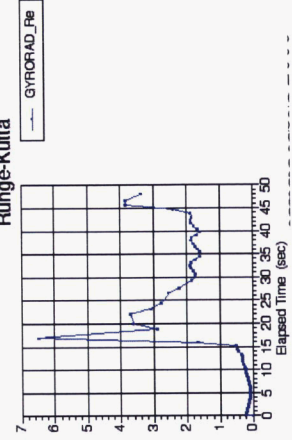
Xsirt = -12 ; Ysirt = +5 ; Zsirt = +1.
 Kp = 3.0 ; EngSirt = 1000 keV
 PAsirt = +20 deg ; AZMsirt = +30 deg
 Runge-Kutta



Xsirt = -12 ; Ysirt = +5 ; Zsirt = +1.
 Kp = 3.0 ; EngSirt = 1000 keV
 PAsirt = +20 deg ; AZMsirt = +30 deg
 Runge-Kutta

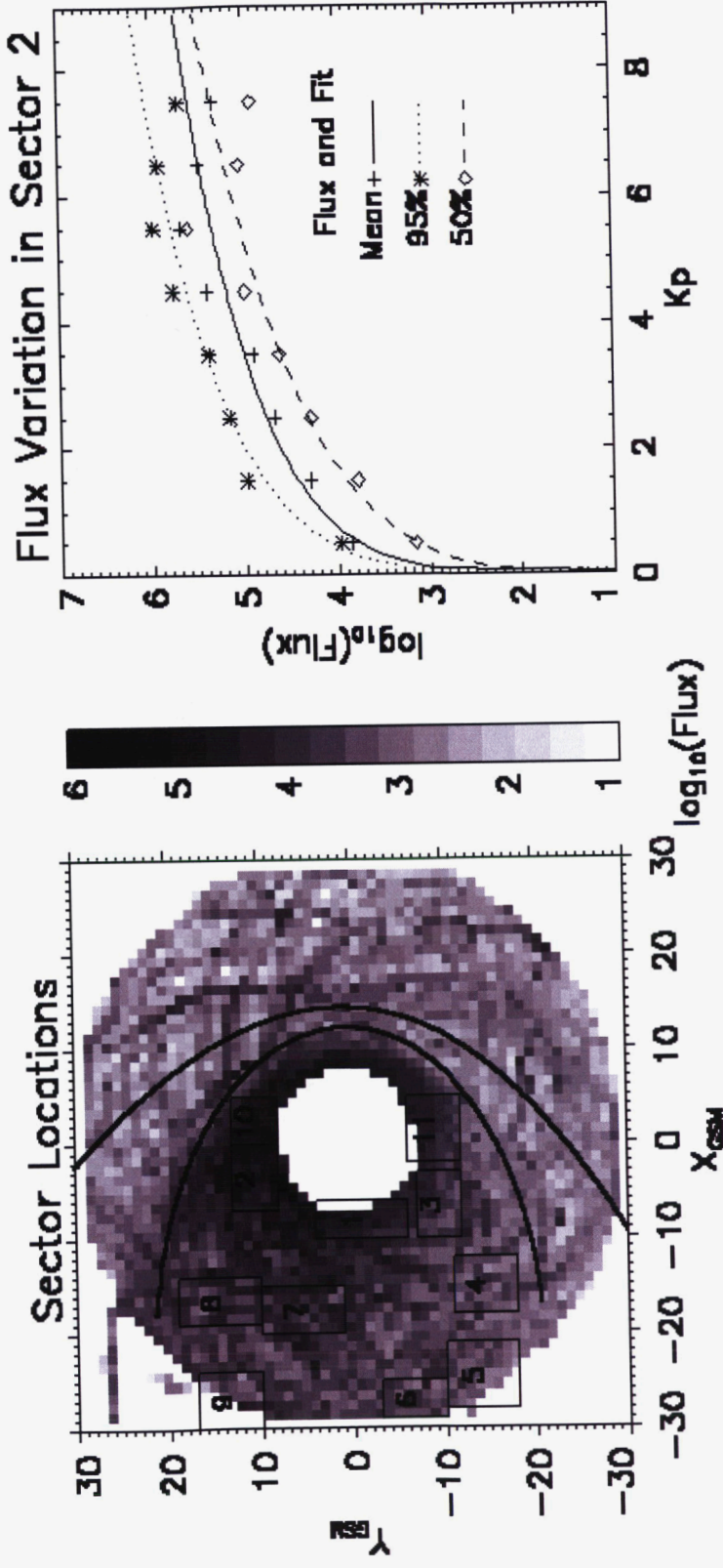


Xsirt = -12 ; Ysirt = +5 ; Zsirt = +1.
 Kp = 3.0 ; EngSirt = 1000 keV
 PAsirt = +20 deg ; AZMsirt = +30 deg
 Runge-Kutta

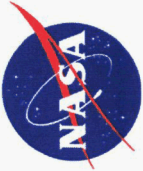




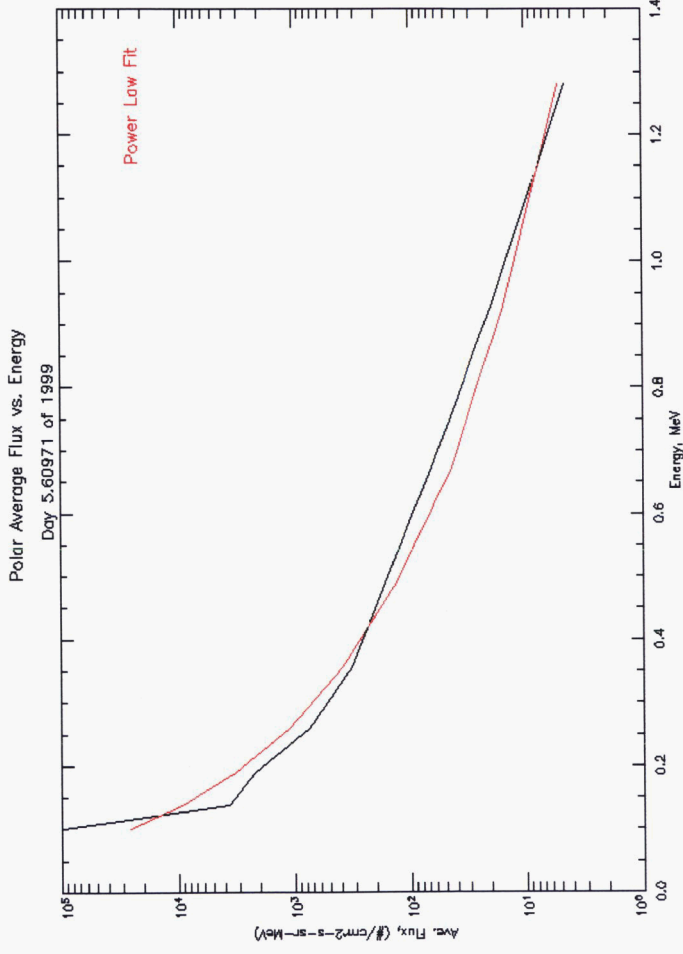
Flux Scaling



- Flux measurements are sparse at large Kp over much of magnetosphere
- Scaling laws are used to scale the mean, 50%, and 95% levels for any Kp value



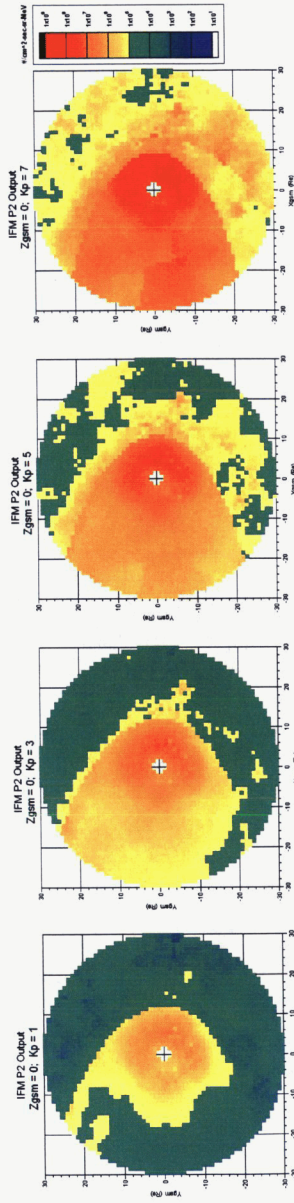
Polar Spacecraft Data



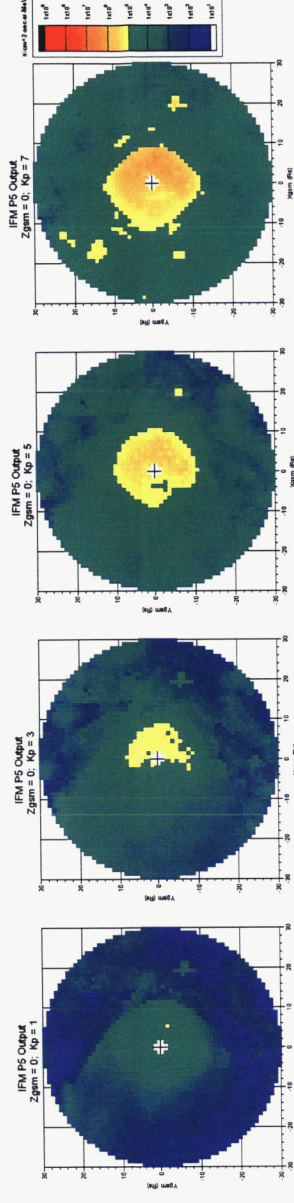
- IFM output energy bins are tied to the Geotail energy bins
- Polar's number and energy limits of data channels differ from Geotail's
 - Power law fit made to the spectrum for each Polar measurement
 - Allows for integration of flux inside each of the Geotail energy bins



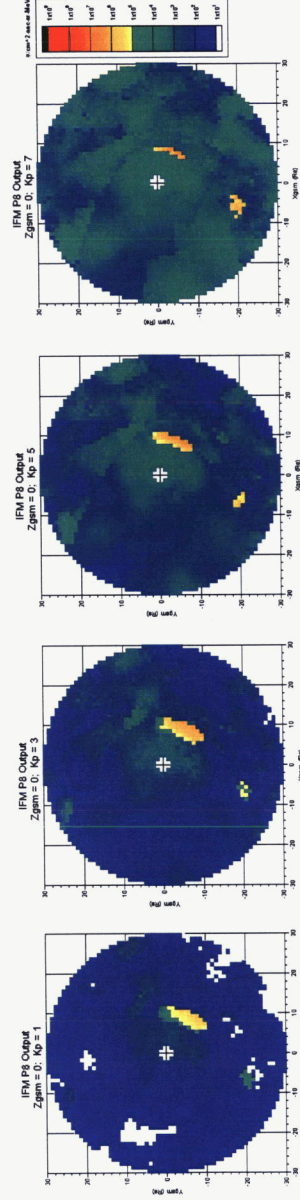
IFM Proton Flux



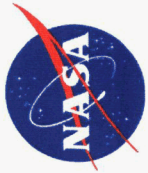
• 58.1 – 77.3 keV



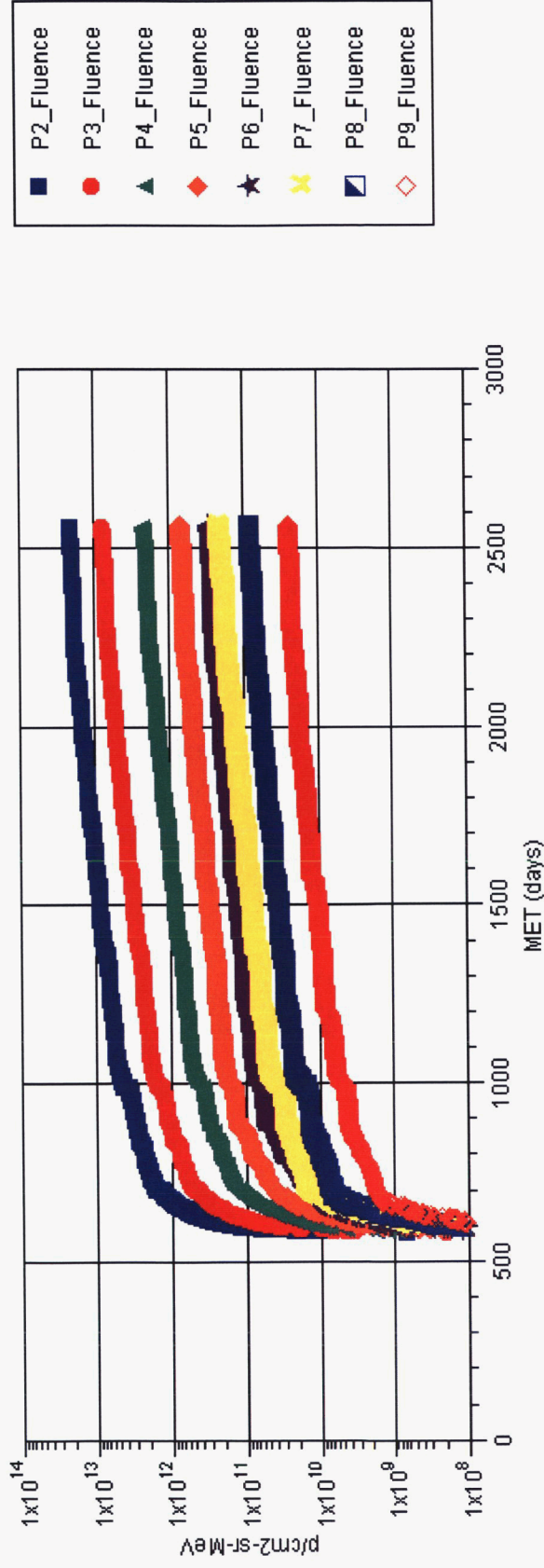
• 154.3 – 227.5 keV



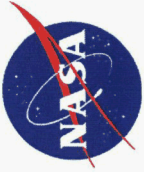
• 522.5 – 813.5 keV



IFM Fluence Calculation



- Chandra ephemeris used in this example
- Mission fluence (#/[cm²-sr-MeV]) calculated for each of the energy channels available in IFM



Summary

- The Living With a Star Ion Flux Model (IFM) is a radiation environment risk mitigation tool
- Incorporates flux observations from the Polar and Geotail S/C
 - Empirical, database driven model of outer magnetosphere, magnetosheath, and solar wind free field ion flux
 - Geocentric distances from 2 to 30 Re
 - Provides differential energy flux from 58.1 to 1560.8 keV
- Provides ion flux predictions for varying geomagnetic disturbance levels represented by the Kp index
- IFM development heavily leveraged experience gained in creating the ion flux model for the Chandra X-ray observatory
 - The Chandra Radiation Model (CRM) is the first engineering-level ion environment model for the outer magnetosphere
 - CRM is designed as a scheduling tool and for real-time estimates of the ion flux environment
 - IFM is more flexible and will have a wider applicability than CRM